



RESEARCH ARTICLE

**REVISED** Theoretical spectroscopic study of acetyl ( $\text{CH}_3\text{CO}$ ), vinyloxy ( $\text{CH}_2\text{CHO}$ ), and 1-methylvinyloxy ( $\text{CH}_3\text{COCH}_2$ ) radicals. Barrierless formation processes of acetone in the gas phase [version 2; peer review: 2 approved]

Hamza El Hadki<sup>1</sup>, Victoria Guadalupe Gámez<sup>2</sup>, Samira Dalbouha<sup>1,3</sup>, Khadija Marakchi<sup>1</sup>, Oum Keltoum Kabbaj<sup>1</sup>, Najia Komiha<sup>1</sup>, Miguel Carvajal <sup>4,5</sup>, Maria Luisa Senent Diez <sup>2</sup>

<sup>1</sup>Laboratoire de Spectroscopie, Modélisation Moléculaire, Matériaux, Nanomatériaux, Eau et Environnement, LS3MN2E/CERNE2D, Faculté des Sciences Rabat, Université Mohammed V, Rabat, BP1014, Morocco

<sup>2</sup>Departamento de Química y Física Teóricas, IEM-CSIC, Unidad Asociada GIFMAN, CSIC-UHU, Madrid, 28006, Spain

<sup>3</sup>Equipe de recherche : Matériaux et Applications Environnementales, Laboratoire de Chimie Appliquée et Environnement, Département de chimie, Faculté des Sciences d'Agadir, Université Ibn Zohr, Agadir, B.P 8106, Morocco

<sup>4</sup>Departamento de Ciencias Integradas, Centro de Estudios Avanzados en Física, Matemática y Computación; Unidad Asociada GIFMAN, CSIC-UHU, Universidad de Huelva, Huelva, 21071, Spain

<sup>5</sup>Instituto Universitario Carlos I de Física Teórica y Computacional, University of Granada, Granada, Spain

**V2** First published: 30 Sep 2021, 1:116  
<https://doi.org/10.12688/openreseurope.14073.1>  
 Latest published: 18 Mar 2022, 1:116  
<https://doi.org/10.12688/openreseurope.14073.2>

### Abstract

**Background:** Acetone is present in the earth's atmosphere and extra-terrestrially. The knowledge of its chemical history in these environments represents a challenge with important implications for global tropospheric chemistry and astrochemistry. The results of a search for efficient barrierless pathways producing acetone from radicals in the gas phase are described in this paper. The spectroscopic properties of radicals needed for their experimental detection are provided.

**Methods:** The reactants were acetone fragments of low stability and small species containing C, O and H atoms. Two exergonic bimolecular addition reactions involving the radicals  $\text{CH}_3$ ,  $\text{CH}_3\text{CO}$ , and  $\text{CH}_3\text{COCH}_2$ , were found to be competitive according to the kinetic rates calculated at different temperatures. An extensive spectroscopic study of the radicals  $\text{CH}_3\text{COCH}_2$  and  $\text{CH}_3\text{CO}$ , as well as the  $\text{CH}_2\text{CHO}$  isomer, was performed. Rovibrational parameters, anharmonic vibrational transitions, and excitations to the low-lying excited states are provided. For this purpose, RCCSD(T)-F12 and MRCI/CASSCF calculations were performed. In addition, since all the species presented non-rigid properties, a variational procedure of reduced dimensionality was employed to explore the far infrared region.

### Open Peer Review

Approval Status

	1	2
<b>version 2</b>		
(revision)		
18 Mar 2022	<a href="#">view</a>	<a href="#">view</a>
<b>version 1</b>		
30 Sep 2021	<a href="#">view</a>	<a href="#">view</a>

1. **Nicola Tasinato**, Scuola Normale Superiore of Pisa, Pisa, Italy
2. **Ha Vinh Lam Nguyen**, University of Paris Est Creteil, Paris, France  
**Isabelle Kleiner**, Université de Paris, Paris, France

Any reports and responses or comments on the article can be found at the end of the article.

**Results:** The internal rotation barriers were determined to be  $V_3=143.7\text{ cm}^{-1}$  ( $\text{CH}_3\text{CO}$ ),  $V_2=3838.7\text{ cm}^{-1}$  ( $\text{CH}_2\text{CHO}$ ) and  $V_3=161.4\text{ cm}^{-1}$  and  $V_2=2727.5\text{ cm}^{-1}$  ( $\text{CH}_3\text{COCH}_2$ ). The splitting of the ground vibrational state due to the torsional barrier have been computed to be  $2.997\text{ cm}^{-1}$ ,  $0.0\text{ cm}^{-1}$ , and  $0.320\text{ cm}^{-1}$ , for  $\text{CH}_3\text{CO}$ ,  $\text{CH}_2\text{CHO}$ , and  $\text{CH}_3\text{COCH}_2$ , respectively.

**Conclusions:** Two addition reactions,  $\text{H}+\text{CH}_3\text{COCH}_2$  and  $\text{CH}_3+\text{CH}_3\text{CO}$ , could be considered barrierless formation processes of acetone after considering all the possible formation routes, starting from 58 selected reactants, which are fragments of the molecule. The spectroscopic study of the radicals involved in the formation processes present non-rigidity. The interconversion of their equilibrium geometries has important spectroscopic effects on  $\text{CH}_3\text{CO}$  and  $\text{CH}_3\text{COCH}_2$ , but is negligible for  $\text{CH}_2\text{CHO}$ .

### Keywords

acetone,  $\text{CH}_3\text{CO}$ ,  $\text{CH}_2\text{CHO}$ ,  $\text{CH}_3\text{COCH}_2$ , radical, spectrum, barrierless, LAM



This article is included in the [Excellent Science gateway](#).



This article is included in the [Analytical Techniques collection](#).

**Corresponding author:** Maria Luisa Senent Diez ([ml.senent@csic.es](mailto:ml.senent@csic.es))

**Author roles:** **El Hadki H:** Data Curation, Investigation; **Gámez VG:** Data Curation, Formal Analysis, Investigation, Resources, Software, Visualization; **Dalbouha S:** Data Curation, Formal Analysis, Investigation, Visualization; **Marakchi K:** Conceptualization, Data Curation, Investigation, Validation; **Kabbaj OK:** Formal Analysis, Supervision, Validation; **Komiha N:** Conceptualization, Formal Analysis, Funding Acquisition, Investigation, Project Administration, Validation; **Carvajal M:** Conceptualization, Funding Acquisition, Investigation, Methodology, Project Administration, Validation, Writing – Original Draft Preparation; **Senent Diez ML:** Conceptualization, Formal Analysis, Funding Acquisition, Investigation, Methodology, Project Administration, Resources, Software, Supervision, Writing – Original Draft Preparation, Writing – Review & Editing

**Competing interests:** No competing interests were disclosed.

**Grant information:** This project has received funding from the European Union's Horizon 2020 research and innovation programme under the Marie Skłodowska-Curie grant agreement No 872081. This work was also supported by the Ministerio de Ciencia, Innovación y Universidades of Spain through the grants EIN2019-103072 and FIS2016-76418-P; the CSIC i-coop+2018 program under the grant number COOPB20364; the CTI (CSIC) and CESGA and to the "Red Española de Computación" for the grants AECT-2020-2-0008 and RES-AECT-2020-3-0011 for computing facilities. MC also acknowledges the financial support from the Spanish National Research, Development, and Innovation plan (RDI plan) under the project PID2019-104002GB-C21 and the Consejería de Conocimiento, Investigación y Universidad, Junta de Andalucía and European Regional Development Fund (ERDF), Ref. SOMM17/6105/UGR. *The funders had no role in study design, data collection and analysis, decision to publish, or preparation of the manuscript.*

**Copyright:** © 2022 El Hadki H *et al.* This is an open access article distributed under the terms of the [Creative Commons Attribution License](#), which permits unrestricted use, distribution, and reproduction in any medium, provided the original work is properly cited.

**How to cite this article:** El Hadki H, Gámez VG, Dalbouha S *et al.* **Theoretical spectroscopic study of acetyl ( $\text{CH}_3\text{CO}$ ), vinoxy ( $\text{CH}_2\text{CHO}$ ), and 1-methylvinoxy ( $\text{CH}_3\text{COCH}_2$ ) radicals. Barrierless formation processes of acetone in the gas phase [version 2; peer review: 2 approved]** Open Research Europe 2022, 1:116 <https://doi.org/10.12688/openreseurope.14073.2>

**First published:** 30 Sep 2021, 1:116 <https://doi.org/10.12688/openreseurope.14073.1>

**REVISED Amendments from Version 1**

We thank the referees for their work he has made and the interest they have shown for the article. Throughout the publication, the following changes have been made in accordance with the comments of the referees.

- 1) Tables and figures have been rearranged. Next to the article we add the new figures, three of them have been reformed according to the comments. We attach files with the figures. They follow the new order.
- 2) In the “computational section” and also in other sections comments concerning the precision of the calculations have been added. As one of the referees emphasizes most of the calculations are predictions and cannot be compared with experimental data. We rely on the results obtained in previous studies of other less unique molecules, carried out with the same methodology. The selected methodology is more accurate for the spectroscopic study than for the reactivity. We emphasize the number of calculations performed for reactivity.
- 3) Intensities have been added to Table 6 (old Table 5). Explanations about the selected theory for the computations of dipole moments were added.
- 4) The main discussion of the referees concerns the rotational constants and the comparison with the experimental data. Explanations have been added. The sentence “Generally, for many molecules the computed  $B_0$  and  $C_0$  are more accurate than  $A_0$ ” refers (only) to the formulae that we employ combining ab initio levels. Of course, many authors follow other procedures with other results. For CH<sub>2</sub>COH, the sentence has been rewritten: “For CH<sub>2</sub>CHO, the agreement between computed and measured rotational constants of  $B_0$  and  $C_0$  was excellent and tolerable in the case of  $A_0$  ( $A_0^{\text{CAL}} - A_0^{\text{EXP}} = 95.3$  MHz,  $B_0^{\text{CAL}} - B_0^{\text{EXP}} = -1.7$  MHz, and  $C_0^{\text{CAL}} - C_0^{\text{EXP}} = 3.2$  MHz)”. We believe that these questions are more clear.
- 5) Typos have been corrected in all the paper.

**Any further responses from the reviewers can be found at the end of the article**

### Plain language summary

In addition to its industrial applications, acetone (CH<sub>3</sub>COCH<sub>3</sub>), the smallest ketone, is present in gas phase environments such as the earth’s atmosphere and extraterrestrial sources. The knowledge of its chemical history in these environments, as well as that of other volatile molecular species, represents a challenge with important implications for global tropospheric chemistry. Organic radicals can play important roles in the chemical evolution.

In this paper gas phase barrierless processes and the corresponding properties were studied at different temperatures. Probable exergonic bimolecular addition processes, which reactants are acetone fragments or small neutral species observed in the gas phase sources containing C, O and H atoms, were described. In addition, this paper is devoted to the theoretical spectroscopic study of three radicals: the acetyl radical (CH<sub>3</sub>CO), the vinoxy radical (CH<sub>2</sub>CHO), and the 1-methylvinoxy radical (CH<sub>3</sub>COCH<sub>2</sub>). The three systems were acetone fragments and potential reactants. Our main objective is to provide the theoretical point of view to help further spectroscopic studies of these not-yet-fully characterized species that can play important roles in the gas phase chemistry.

### Introduction

In addition to its industrial applications, acetone (CH<sub>3</sub>COCH<sub>3</sub>), the smallest ketone, is present in gas phase environments such as the earth’s atmosphere and the interstellar medium<sup>1-5</sup>. The knowledge of its chemical history in these environments, as well as that of other volatile molecular species, represents a challenge with important implications for global tropospheric chemistry and astrochemistry. Organic radicals can play important roles in the chemical evolution of the terrestrial atmosphere and extra-terrestrial gas phase sources.

Atmospheric acetone arises from both natural and anthropogenic sources<sup>1,2</sup>. It is naturally produced by vegetation that emits large quantities of nonmethane organic compounds. In the troposphere, these biogenic compounds can undergo photolysis and react with OH and NO<sub>3</sub> radicals, and ozone, resulting in the formation of oxygenated products such as ketones<sup>2,5,6</sup>. On the other side, acetone is a major source of hydrogen oxide radicals (HO<sub>x</sub>) and peroxyacetyl nitrate through photolysis<sup>2,6</sup>. Decomposition of acetone can occur in the presence of OH to produce radicals such as CH<sub>3</sub>COCH<sub>2</sub><sup>7</sup>. The OH-initiated oxidation of acetone in the presence of NO in air has been shown to form the acetonoxyl radical [CH<sub>3</sub>COCH<sub>2</sub>O], which undergoes rapid decomposition under atmospheric conditions to form HCHO and CH<sub>3</sub>CO<sup>1</sup>.

Acetone was the first ten-atom molecule to be detected in the interstellar medium<sup>4,5</sup>. Recently, it has been observed in the gas phase in various extraterrestrial environments<sup>8,9</sup>. It is generally accepted that organic compounds are formed in the interstellar medium on ice mantles, although the possibility of gas phase processes

is not ignored<sup>10</sup>. At the temperatures and pressures of the interstellar medium, barrierless processes can be competitive with respect to those involving ice mantles<sup>11</sup>. Barrierless processes involve low stability species such as radicals, charged or unsaturated molecules<sup>11</sup>.

Following the same methodology employed in a previous work<sup>11</sup>, for this paper, gas phase barrierless processes and the corresponding kinetic rates were studied at different temperatures. Probable exergonic bimolecular addition processes, the reactants which are acetone fragments or small neutral species observed in the gas phase sources containing C, O and H atoms, are described. In addition, this paper is devoted to the theoretical spectroscopic study of three radicals: the acetyl radical ( $\text{CH}_3\text{CO}$ ), the vinoxy radical ( $\text{CH}_2\text{CHO}$ ), and the 1-methylvinoxy radical ( $\text{CH}_3\text{COCH}_2$ ). The three systems were acetone fragments and potential reactants. Our main objective is to provide perspective from the *ab initio* calculations and to help further spectroscopic studies of these three, not yet fully characterized species that can play important roles in the gas phase chemistry involving organic molecules, such as diacetyl or pyruvic acid<sup>12,13</sup>.

The rotational spectra of  $\text{CH}_3\text{CO}$  and  $\text{CH}_2\text{CHO}$  were measured by Hirota *et al.*<sup>14</sup>, Endo *et al.* and Hansen *et al.*<sup>15,16</sup>, respectively. As far as we know, experimental rotational parameters are not available for  $\text{CH}_3\text{COCH}_2$ .

The vibrational spectra of the  $\text{CH}_3\text{CO}$ ,  $\text{CH}_2\text{CHO}$ , and  $\text{CH}_3\text{COCH}_2$  radicals were studied in Ar matrices by Jacox<sup>17</sup>, Shirk *et al.*<sup>18</sup>, and Lin *et al.*<sup>19</sup>, respectively, whereas Das and Lee<sup>20</sup> addressed the infrared spectrum of  $\text{CH}_3\text{CO}$  in solid p- $\text{H}_2$ . In the gas phase, previous measurements corresponding to  $\text{CH}_2\text{CHO}$ <sup>21–27</sup> and  $\text{CH}_3\text{COCH}_2$ <sup>28</sup> are accessible, whereas for  $\text{CH}_3\text{CO}$  experimental vibrational data in the gas phase are unavailable.

Low-lying electronic transitions were previously measured for the three radicals. The  $\text{CH}_3\text{CO}$  radical photodecomposes into  $\text{CH}_3+\text{CO}$  in the visible region<sup>17</sup>. The ground electronic state presented a doublet multiplicity character. In addition, three excited electronic doublet states have been explored<sup>29–32</sup>. Band centers were determined to lie at 2.3 eV<sup>29</sup> and in the 200–240 nm (5.1–6.2 eV) region<sup>30</sup>. Maricq *et al.*<sup>31</sup> observed bands at 217 nm (2.3 eV) and in the 240–280 nm (4.4–5.1 eV) region, which were confirmed by Cameron *et al.*<sup>32</sup>. For the  $\text{CH}_2\text{CHO}$  isomer, the  $\text{A}(\text{A}'')\leftarrow\text{X}(\text{A}'')$  and  $\text{B}(\text{A}'')\leftarrow\text{X}(\text{A}'')$  transitions have been centered at 1.0 eV<sup>26,33,34</sup> and at 3.6 eV<sup>22–25,33,35,36</sup> using different experimental techniques. The  $\text{B}(\text{A}'')\leftarrow\text{X}(\text{A}'')$  transition of  $\text{CH}_3\text{COCH}_2$  was found at 3.4 eV by Williams *et al.*<sup>37,38</sup> who also provided internal rotation barriers. To our knowledge, all the previous experimental data concerned doublet states. No information is available concerning quartet states. Since one of our objectives was to localize the excited states, all the previous data is summarized with our results.

Theoretical techniques have also been applied to the study of the three radicals<sup>39–41</sup>. Mao *et al.*<sup>39</sup> have determined vertical excitation energies to four excited doublet states of  $\text{CH}_3\text{CO}$  using multireference single and double excitation configuration interaction. The work of Yamaguchi *et al.*<sup>40</sup> focused on the excited electronic states of  $\text{CH}_2\text{CHO}$ , and  $\text{CH}_3\text{COCH}_2$  radicals, was performed using multireference configuration interaction theory.

For this new paper, we tackle to different spectroscopic properties with special attention to the far infrared region, relevant for the interpretation of rovibrational spectra. This new paper is organized as follows: The “computational tools” section under the Methods contains information about the electronic structure computations and computer codes. The next section presents the results and the discussion about the barrierless formation processes of acetone and the corresponding kinetic rates; the spectroscopic characterization of the radicals using two different procedures (one of them suitable for species with large amplitude vibrations and the far infrared region) is explored. Our recent studies of acetone<sup>42</sup> and the  $\text{CH}_3\text{OCH}_2$  radical<sup>43</sup> are examples of this last procedure. Finally, the conclusions are drawn.

## Methods

### Computational tools

Different levels of electronic structure theory were combined taking into consideration the computational requirements of the reactive processes and the spectroscopic studies.

**Formation processes.** The search for the possible barrierless formation processes was performed using the Searching Tool for Astrochemical Reactions (STAR) online tool<sup>44</sup>. This statistical tool contains a broad and comprehensive molecular database. Implemented algorithms search for all the likely combinations of reactants leading to a specific molecular species. The processes producing the desired molecule and some subproducts are automatically rejected if the viability of these last species cannot be confirmed according to the Gibbs free energy. The viability is considered confirmed when species are listed in the data base. The corresponding minimum energy paths were computed using the density functional theory (DFT)<sup>45</sup> and the

6-311+G(d,p) basis set<sup>46</sup> as it is implemented in the GAUSSIAN 16 software<sup>47</sup>. The thermochemical properties were determined by optimizing the geometry with the CBS-QB3 procedure<sup>48</sup>, a complete basis set model implemented in GAUSSIAN modified for the use of the B3LYP hybrid density functional. The corresponding kinetic rate constants were computed using POLYRATE version 2017 software<sup>49</sup>. This procedure provides a qualitative description suitable for elucidating what processes can follow barrierless paths. It allows compare thermodynamic and kinetic parameters in different processes and to select the most probable reactions.

**Spectroscopic and geometrical properties.** The ground electronic state structure of the three radicals and the corresponding harmonic frequencies were computed using explicitly correlated coupled cluster theory with single and double substitutions, augmented by a perturbative treatment of triple excitations, RCCSD(T)-F12<sup>50,51</sup> implemented in MOLPRO version 2012.1<sup>52</sup>. The default options and a basis set denoted by AVTZ-F12, were employed. AVTZ-F12 contains the aug-cc-pVTZ (AVTZ)<sup>53</sup> atomic orbitals, the corresponding functions for the density fitting, and the resolutions of the identity. The core-valence electron correlation effects on the rotational constants were introduced using RCCSD(T)<sup>54</sup> and the cc-pCVTZ basis set (CVTZ)<sup>55</sup>. The ability of these methods for determining accurate geometries is well known. In the section dedicated to describe rotational parameters, references of previous applications are provided and discussed. RCCSD(T)-F12/AVTZ provides results of the same accuracy than RCCSD(T)/AV5Z.

The three radicals can be defined as nonrigid molecules because they show large amplitude motions that interconvert different minima of the potential energy surface (PES). Then, two different theoretical models were combined to determine the spectroscopic parameters, vibrational second order perturbation theory (VPT2)<sup>56</sup> implemented in GAUSSIAN, and a variational procedure of reduced dimensionality which is detailed in our papers<sup>57-59</sup>.

If VPT2 is applied, a unique minimum is postulated to exist in the potential energy surfaces, the radicals are assumed to be semi-rigid and all the vibrations are described as small displacements around the equilibrium geometry. For  $\text{CH}_3\text{CO}$ ,  $\text{CH}_2\text{CHO}$ , and  $\text{CH}_3\text{COCH}_2$ , anharmonic spectroscopic frequencies were obtained from anharmonic force fields, computed using second order and two basis sets: the VQZ (for  $\text{CH}_3\text{CO}$  and  $\text{CH}_2\text{CHO}$ ), and the AVTZ (for  $\text{CH}_3\text{COCH}_2$ )<sup>52</sup>.

If the variational procedure is applied, the non-rigidity is taken into account and the minimum interconversion is considered implicitly. For this purpose, RCCSD(T)-F12/AVTZ potential energy surfaces were computed, and later on they were vibrationally using MP2 and two basis sets: the VQZ (for  $\text{CH}_3\text{CO}$  and  $\text{CH}_2\text{CHO}$ ), and the AVTZ (for  $\text{CH}_3\text{COCH}_2$ ).

Vertical excitation energies to the excited electronic states were computed using MRCI/CASSCF theory<sup>60,61</sup>. For the two small radicals, the active space was constructed with eight a' and four a'' orbitals and 13 electrons. The five a' internal orbitals, doubly occupied in all the configurations, were optimized. In the case of  $\text{CH}_3\text{COCH}_2$ , the active space was built using nine a' and four a'' orbitals and fifteen electrons, whereas eight a' orbitals were optimized but they were doubly occupied in all the configurations. With respect to the accuracy of these calculations, we stand out that we have computed vertical excitations. Then the energies are overestimated with respect to the measurements.

## Results and discussion

### Barrierless formation processes of acetone: the function of radicals

In the gas phase, efficient reactions for competing with formation processes on ice surfaces are those which follow barrierless pathways and involve low stability species. To establish some limits to the present work, we choose the set of reactants shown in Table 1. In principle, they obey the following conditions: (1) they enclose the atomic elements H, C, and O constituents of acetone; (2) they contain at most eleven atoms, as the objective is to select chemical routes of increasing molecular complexity; (3) they have been detected in the gas phase of the ISM or, at least, they are listed as probable detectable species. We detail this procedure in our previous paper on the  $\text{C}_3\text{O}_3\text{H}_6$  isomers<sup>11</sup>.

All the possible chemical routes starting from the selected reactants were automatically generated by the STAR software<sup>44</sup>. This statistical tool contains a broad and comprehensive molecular database. Implemented algorithms search for all likely combinations of reactants leading to a specific molecular species. The processes producing the desired molecule and some by-products are automatically rejected if the viability of these last species cannot be confirmed. The tool selects the exergonic processes for which the exchange of Gibbs free energies is negative ( $\Delta G < 0$ ). The selected processes must occur following a limited number of steps. The number of steps is considered to concur with the sum of breaking and forming bonds. To quantify them, the maximum number of necessary elementary steps (MNES) parameter is defined.

**Table 1.** List of selected reactants ( $N_a$  = number of atoms).

$N_a$	Reactants
1	$\cdot\text{H}$
2	$\text{H}_2$ ; $^3\text{O}_2$ ; $\text{C}_2$ ; $\text{OH}\cdot$ ; $\text{CH}\cdot$ ; $\text{OH}^+$ ; $\text{CH}^+$ ; $\text{CO}\cdot$ ; $\text{CO}$
3	$\text{C}_3$ ; $\text{HOC}\cdot$ ; $\text{C}_2\text{H}\cdot$ ; $\text{H}_2\text{O}$ ; $\text{C}_2\text{O}$ ; $\text{H}_2\text{O}\cdot$ ; $^3\text{CH}_2$ ; $\text{H}_3^+$ ; $\text{CO}_2$ ; $\text{HCO}^+$ ; $\text{HCO}\cdot$
4	$\text{HOCO}^+$ ; $\text{I-C}_3\text{H}\cdot$ ; $\text{CH}_3\cdot$ ; $\text{H}_2\text{CO}$ ; $\text{HCOH}$ ; $\text{C}_3\text{O}$ ; $\text{HCOO}\cdot$ ; $\text{C}_2\text{H}_2$ ; $\text{HOCO}\cdot$ ; $\text{H}_3\text{O}^+$ ; $\text{HCCO}$
5	$\cdot\text{CH}_2\text{OH}$ ; $\text{C}_4\text{H}\cdot$ ; $\text{CH}_3\text{O}\cdot$ ; $\text{C}_4\text{H}$ ; $\text{HCOOH}$ ; $\text{CH}_4$ ; $\text{I-C}_3\text{H}_2$ ; $\text{CH}_2\text{CO}$
6	$\text{C}_2\text{H}_4$ ; $\text{CH}_3\text{CO}\cdot$ ; $\text{CH}_3\text{OH}$ ; $\cdot\text{CH}_2\text{CHO}$ ; $\text{HC}_2\text{CHO}$ ; $\text{H}_2\text{C}_4$ ; $\text{HC}_4\text{H}$
7	$\text{CH}_3\text{CHO}$ ; $\text{CH}_2\text{CHOH}$ ; $\text{CH}_3\text{C}_2\text{H}$
8	$\text{CH}_2\text{CHCHO}$ ; $\text{CH}_3\text{OCH}_2\cdot$ ; $\text{CH}_3\text{CHOH}$
9	$\text{CH}_3\text{C}_4\text{H}$ ; $\text{CH}_3\text{CH}_2\text{OH}$ ; $\text{CH}_3\text{COCH}_2\cdot$ ; $\text{CH}_3\text{CCH}_3$ ; $\text{CH}_3\text{CHCH}_2$

In principle, 75 exergonic processes were derived from STAR (see Table 2). For all of them,  $\Delta G$  was computed by optimizing the geometry using the CBS-QB3 procedure<sup>48</sup>. Fourteen final exergonic reactions for which  $\text{MNES} < 3$  were found, but only two of them could be considered as barrierless processes (see Table 3). Energy profiles proving these findings were computed at the M05-2X/6-311+G(d,p) level of theory<sup>45,46</sup>. They represent minimum energy paths (see Figure 1).

The kinetic rate constants of the processes are summarized in Table 3. They were evaluated using the single-faceted variable-reaction-coordinate variational transition state theory (VRC-VTST)<sup>62,63</sup> implemented in POLYRATE<sup>49</sup>. The rate constants obey the following equation:

$$k(T, s) = \frac{\hbar^2}{2\pi} g_e \frac{\sigma_1 \sigma_2}{\sigma^\ddagger Q_1 Q_2} \left( \frac{2\pi}{\mu k_B T} \right)^{3/2} \int dE e^{-E/k_B T} dJ N(E, J, s) \quad (1)$$

In this equation,  $s$  and  $T$  denote the reaction coordinate and the temperature, respectively;  $g_e$  represents the rate between the electronic partition function of the transition state and the product of the electronic partition function of the two reactants;  $\mu$ ,  $Q_1$  and  $Q_2$  designate the reduced mass and the rotational partition functions of the reactants.  $J$  is the angular momentum quantum number and  $N(E, J, s)$  represents the number of allowed states corresponding to the  $E$  energy.  $\sigma_1$ ,  $\sigma_2$ , and  $\sigma^\ddagger$  denote the cross-sections of the two reactants and of the transition states.

The starting points of the rate computation were the M05-2X/6-311+G(d,p) energies, geometries and harmonic fundamentals of reactants and products computed along the pathways. The  $s$  reaction coordinate was allowed to vary from 1.8 to 4.2 Å with intervals of 0.2 Å. The rates were computed at fifteen different  $T$  (200, 210, 220, 230, 240, 250, 260, 280, 298, 300, 400, 500, 700, 900 and 1000K). The number of allowed states was determined in a Monte Carlo simulation considering all the possible orientations. The rates at 200K (middle point of the interstellar Hot Core temperature range, 100-300K), 298K (room temperature), and 500K, corresponding to the 2 barrierless processes, are shown in Table 3. Rates were computed using the canonical variational transition state theory (CVT), which is the conventional theory. However, as CVT is not recommended for very low temperatures, rates at 200K were also computed using microcanonical variational transition state theory ( $\mu\text{VT}$ ) with multidimensional semiclassical approximations for tunneling and nonclassical reflection<sup>64,65</sup>.

### Spectroscopic characterization of $\text{CH}_3\text{CO}$ , $\text{CH}_2\text{CHO}$ , and $\text{CH}_3\text{COCH}_2$

**Ground electronic state: equilibrium structures.** The study of the rovibrational properties of acetone and its monosubstituted isotopologues using *ab initio* calculations was the aim of a previous work from some of the authors of the present paper<sup>42</sup>. In this new paper, we attend, using a similar methodology, the structural and spectroscopic parameters of the three radicals,  $\text{CH}_3\text{CO}$ ,  $\text{CH}_2\text{CHO}$ , and  $\text{CH}_3\text{COCH}_2$ , involved in acetone gas phase processes.

Table 4 collects the RCCSD(T)-F12/AVTZ structural parameters and the equilibrium rotational constants of the preferred geometries of the three radicals in their ground electronic state. The three geometries can

**Table 2. Exergonic reactions with reactants ( $\Delta G$ , in kcal/mol, at 10K and 0.1atm at CBS-QB3 level of theory; MNES is the maximum number of necessary elementary steps).**

	Reactions	$\Delta G$	MNES
1	$H\cdot + CH_3COCH_2 \rightarrow CH_3COCH_3$	-94.9	1
2	$CH_3\cdot + CH_3CO\cdot \rightarrow CH_3COCH_3$	-83.4	1
3	$CH_3\cdot + \cdot CH_2CHO \rightarrow CH_3COCH_3$	-89.2	2
4	$HCO\cdot + CH_3COCH_2 \rightarrow CH_3COCH_3 + CO$	-80.6	2
5	$CH_3O\cdot + CH_3COCH_2 \rightarrow CH_3COCH_3 + H_2CO$	-75.8	2
6	$CH_2OH\cdot + CH_3COCH_2 \rightarrow CH_3COCH_3 + H_2CO$	-67.3	2
7	$CHOH + CH_3COCH_2 \rightarrow CH_3COCH_3 + HCO\cdot$	-60.3	2
8	$\cdot CH_2CHO + CH_3COCH_2 \rightarrow CH_3COCH_3 + CH_2CO$	-59.1	2
9	$CH_3CO\cdot + CH_3COCH_2 \rightarrow CH_3COCH_3 + CH_2CO$	-53.3	2
10	$HOCO+ + CH_3CCH_3 \rightarrow CH_3COCH_3 + HOC+$	-32.3	2
11	$HC_2CHO + CH_3CCH_3 \rightarrow CH_3COCH_3 + I-C_3H_2$	-24.0	2
12	$I-H_2C_4 + CH_3COCH_2 \rightarrow CH_3COCH_3 + C_4H\cdot$	-8.9	2
13	$H_2CO + CH_3COCH_2 \rightarrow CH_3COCH_3 + HCO\cdot$	-7.4	2
14	$I-C_3H_2 + CH_3COCH_2 \rightarrow CH_3COCH_3 + I-C_3H\cdot$	-4.6	2
15	${}^3CH_2 + CH_3CHO \rightarrow CH_3COCH_3$	-104.9	3
16	$CH_2CO + CH_3CHO \rightarrow CH_3COCH_3 + CO$	-27.2	4
17	$CH_4 + CH_2CO \rightarrow CH_3COCH_3$	-21.1	4
18	$CH_3O\cdot + CH_3CHOH \rightarrow CH_3COCH_3 + H_2O$	-101.5	4
19	$CH_2OH\cdot + CH_3CHOH \rightarrow CH_3COCH_3 + H_2O$	-92.9	4
20	$CH_2OH\cdot + CH_3CCH_3 \rightarrow CH_3COCH_3 + CH_3\cdot$	-86.5	4
21	$CH_2CHOH + CH_3CCH_3 \rightarrow CH_3COCH_3 + C_2H_4$	-83.0	4
22	$CH_3\cdot + CH_3CHOH \rightarrow CH_3COCH_3 + H_2$	-75.3	4
23	$CH_3CHO + CH_3CCH_3 \rightarrow CH_3COCH_3 + C_2H_4$	-72.4	4
24	$HOCO\cdot + CH_3CCH_3 \rightarrow CH_3COCH_3 + HCO\cdot$	-71.2	4
25	$HOCO+ + CH_3CCH_3 \rightarrow CH_3COCH_3 + HCO+$	-70.0	4
26	$HCOOH + CH_3CCH_3 \rightarrow CH_3COCH_3 + H_2CO$	-61.5	4
27	$CHOH + CH_3CCH_3 \rightarrow CH_3COCH_3 + {}^3CH_2$	-57.2	4
28	$CH_3COOH + CH_3CCH_3 \rightarrow CH_3COCH_3 + CH_2CHOH$	-51.1	4
29	$CH_3O\cdot + CH_3CHCH_2 \rightarrow CH_3COCH_3 + CH_3\cdot$	-27.4	4
30	$C_6H\cdot + CH_3CHOH \rightarrow CH_3COCH_3 + C_5$	-26.5	4
31	$CH_3OH + CH_3CHO \rightarrow CH_3COCH_3 + H_2O$	-21.7	4
32	$OH\cdot + CH_3CHCH_2 \rightarrow CH_3COCH_3 + H\cdot$	-14.8	4
33	$CH_3O\cdot + CH_3CHO \rightarrow CH_3COCH_3 + OH\cdot$	-7.7	4
34	$CH_3CHO + \cdot CH_2CHO \rightarrow CH_3COCH_3 + HCO\cdot$	-5.7	4
35	$CH_3CHO + CH_3CHCH_2 \rightarrow CH_3COCH_3 + C_2H_4$	-4.7	4
36	$CH_3CHO + CH_3CHOH \rightarrow CH_3COCH_3 + CH_2OH\cdot$	-2.8	4
37	$CH_3CCH + CH_3CHO \rightarrow CH_3COCH_3 + C_2H_2$	-1.8	4
38	$CH\cdot + CH_3CHOH \rightarrow CH_3COCH_3$	-179.6	5
39	$CH_3OH + CH_3CCH_3 \rightarrow CH_3COCH_3 + CH_4$	-94.9	5
40	$HOCO\cdot + CH_3COCH_2 \rightarrow CH_3COCH_3 + CO_2$	-94.6	2

	Reactions	$\Delta G$	MNES
41	${}^3\text{CH}_2 + \text{CH}_3\text{CHOH} \rightarrow \text{CH}_3\text{COCH}_3 + \text{H}\cdot$	-80.8	5
42	$\text{H}_2\text{O} + \text{CH}_3\text{CCH} \rightarrow \text{CH}_3\text{COCH}_3$	-37.8	5
43	$\text{I-C}_3\text{H}_2 + \text{CH}_3\text{CHOH} \rightarrow \text{CH}_3\text{COCH}_3 + \text{C}_2\text{H}\cdot$	-35.9	5
44	$\text{C}_4\text{H}\cdot + \text{CH}_3\text{CHOH} \rightarrow \text{CH}_3\text{COCH}_3 + \text{C}_3$	-33.8	5
45	$\text{H}_2\text{C}_6 + \text{CH}_3\text{CHOH} \rightarrow \text{CH}_3\text{COCH}_3 + \text{C}_5\text{H}\cdot$	-32.7	5
46	$\text{CH}_2\text{CO} + \text{CH}_3\text{COOH} \rightarrow \text{CH}_3\text{COCH}_3 + \text{CO}_2$	-31.7	5
47	$\text{C}_2\text{H}_2 + \text{CH}_3\text{COOH} \rightarrow \text{CH}_3\text{COCH}_3 + \text{CO}$	-30.7	5
48	$\text{CH}_3\text{OH} + \text{CH}_3\text{CHCH}_2 \rightarrow \text{CH}_3\text{COCH}_3 + \text{CH}_4$	-27.3	5
49	$\text{I-H}_2\text{C}_4 + \text{CH}_3\text{COOH} \rightarrow \text{CH}_3\text{COCH}_3 + \text{C}_3\text{O}$	-24.8	5
50	$\text{CH}_2\text{OH}\cdot + \text{CH}_3\text{CHCH}_2 \rightarrow \text{CH}_3\text{COCH}_3 + \text{CH}_3\cdot$	-18.8	5
51	$\text{CH}_2\text{CHOH} + \text{CH}_3\text{CO}\cdot \rightarrow \text{CH}_3\text{COCH}_3 + \text{HCO}\cdot$	-10.5	5
52	${}^3\text{CH}_2 + \text{CH}_3\text{CH}_2\text{OH} \rightarrow \text{CH}_3\text{COCH}_3 + \text{H}_2$	-91.4	6
53	$\text{C}_2\text{H}_4 + \text{CHOH} \rightarrow \text{CH}_3\text{COCH}_3$	-89.9	6
54	$\text{CH}\cdot + \text{CH}_3\text{CH}_2\text{OH} \rightarrow \text{CH}_3\text{COCH}_3 + \text{H}\cdot$	-85.7	6
55	$\text{CHOH} + \text{CH}_3\text{CHOH} \rightarrow \text{CH}_3\text{COCH}_3 + \text{OH}\cdot$	-55.6	6
56	$\text{I-H}_2\text{C}_4 + \text{CH}_3\text{CHOH} \rightarrow \text{CH}_3\text{COCH}_3 + \text{I-C}_3\text{H}\cdot$	-22.6	6
57	$\text{CH}_2\text{OHCHO} + \text{CH}_3\text{CO}\cdot \rightarrow \text{CH}_3\text{COCH}_3 + \text{OHCO}\cdot$	-17.4	6
58	$\text{CH}_2\text{CO} + \text{CH}_3\text{CHOH} \rightarrow \text{CH}_3\text{COCH}_3 + \text{HCO}\cdot$	-17.4	6
59	$\text{C}_2\text{H}_4 + \text{CH}_3\text{CHOH} \rightarrow \text{CH}_3\text{COCH}_3 + \text{CH}_3\cdot$	-16.9	6
60	$\text{CH}_2\text{CHOH} + \text{CH}_3\text{CHCH}_2 \rightarrow \text{CH}_3\text{COCH}_3 + \text{C}_2\text{H}_4$	-15.3	6
61	$\text{I-C}_3\text{H}\cdot + \text{CH}_3\text{CHOH} \rightarrow \text{CH}_3\text{COCH}_3 + \text{C}_2$	-14.7	6
62	$\text{CH}_2\text{CHOH} + \text{CH}_3\text{CHOH} \rightarrow \text{CH}_3\text{COCH}_3 + \text{CH}_2\text{OH}\cdot$	-13.4	6
63	$\text{CH}_2\text{OHCHO} + \text{CH}_3\text{CHCH}_2 \rightarrow \text{CH}_3\text{COCH}_3 + \text{CH}_2\text{CHOH}$	-10.4	6
64	$\text{CH}_3\text{CCH} + \text{CH}_3\text{COOH} \rightarrow \text{CH}_3\text{COCH}_3 + \text{CH}_2\text{CO}$	-5.3	6
65	$\text{H}_2\text{CO} + \text{CH}_3\text{CHOH} \rightarrow \text{CH}_3\text{COCH}_3 + \text{OH}\cdot$	-2.7	6
66	$\text{HOCO} + \text{CH}_3\text{CHCH}_2 \rightarrow \text{CH}_3\text{COCH}_3 + \text{HCO}\cdot$	-2.4	6
67	$\text{H}_2\text{CO} + \text{C}_2\text{H}_4 \rightarrow \text{CH}_3\text{COCH}_3$	-36.8	7
68	$\text{CH}_3\text{CH}_2\text{OH} + \text{CHCO} \rightarrow \text{CH}_3\text{COCH}_3 + \text{HCO}\cdot$	-28.5	7
69	$\text{CH}_3\text{O}\cdot + \text{C}_2\text{H}_4 \rightarrow \text{CH}_3\text{COCH}_3 + \text{H}\cdot$	-17.7	7
70	$\text{CH}_2\text{CHOH} + \text{CH}_3\text{CHOH} \rightarrow \text{CH}_3\text{COCH}_3 + \text{CH}_3\text{O}\cdot$	-4.8	7
71	$\text{H}_2\text{O} + \text{CH}_3\text{CHCH}_2 \rightarrow \text{CH}_3\text{COCH}_3 + \text{H}_2$	-1.3	7
72	$\text{C}_2\text{H}_2 + \text{CH}_3\text{OH} \rightarrow \text{CH}_3\text{COCH}_3$	-57.8	8
73	$\text{CH}_2\text{OHCHO} + \text{CH}_3\text{CHCH}_2 \rightarrow \text{CH}_3\text{COCH}_3 + \text{CH}_3\text{CHO}$	-21.0	8
74	$\text{C}_2\text{H}_4 + \text{CH}_3\text{OH} \rightarrow \text{CH}_3\text{COCH}_3 + \text{H}_2$	-18.2	8
75	$\text{CH}_2\text{OH}\cdot + \text{C}_2\text{H}_4 \rightarrow \text{CH}_3\text{COCH}_3 + \text{H}\cdot$	-9.2	8

**Table 3. Rate constants ( $\text{cm}^3\text{molecule}^{-1}\text{s}^{-1}$ ).**

	Reaction	200K		298K	500K	1000K
		CVT	$\mu\text{VT}$	CVT	CVT	CVT
1	$\text{H}\cdot + \text{CH}_3\text{COCH}_2 \rightarrow \text{CH}_3\text{COCH}_3$	6.3E-21	0.0E+00	2.6E-17	8.2E-15	5.2E-13
2	$\text{CH}_3\cdot + \text{CH}_3\text{CO}\cdot \rightarrow \text{CH}_3\text{COCH}_3$	6.0E-21	0.0E+00	2.4E-17	2.3E-14	3.3E-12

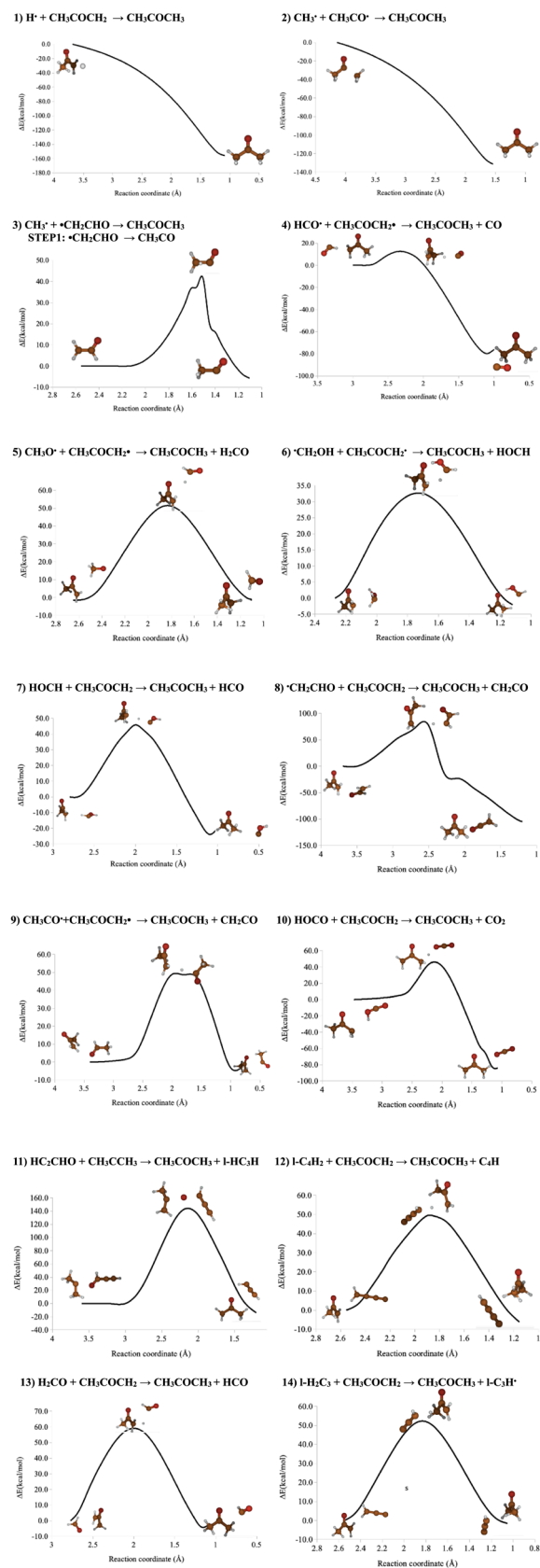


**Figure 1.** Minimum Energy Paths (MEP) corresponding to the formation processes of acetone computed at the M052X/6-31+G(d,p) level of theory.

**Table 4. RCCSD(T)-F12/AVTZ relative energies ( $E$ ,  $E^{\text{ZPVE}}$ , in  $\text{cm}^{-1}$ ), internal rotation barriers ( $V_3$ ,  $V_2$ , in  $\text{cm}^{-1}$ ). Rotational constants (in MHz), MRCI/CASSCF/AVTZ dipole moment (in D) and equilibrium structural parameters (distances, in  $\text{\AA}$ , angles, in degrees) of acetyl, vinyloxy, and 1-methylvinyloxy radicals.**

	$\text{CH}_2\text{CO}^{\text{a}}$ ( $\text{\AA}^2\text{A}'$ )	$\text{CH}_2\text{CHO}$ ( $\text{\AA}^2\text{A}''$ )	$\text{CH}_3\text{COCH}_2^{\text{b}}$ ( $\text{\AA}^2\text{A}''$ )
$E$	0.0	2514.2	-
$E^{\text{ZPVE}}$	0.0	2498.8	-
$V_2$	-	3838.7	2727.5
$V_3$	143.7	-	161.4
$A_e$	84134.35	67084.88	10934.76
$B_e$	9982.57	11456.25	9115.74
$C_e$	9444.29	9785.20	5128.93
$\mu_a$	0.2423	0.9465	0.5444
$\mu_b$	2.3244	2.6175	1.3272
$\mu_c$	0.0	0.0	0.0
$\mu$	2.3281	2.7834	1.4346
<b><math>\text{CH}_3\text{CO}</math></b>		<b><math>\text{CH}_2\text{CHO}</math></b>	
C1C2	1.5116	C1C2	1.4325
O3C1	1.1816	O3C2	1.2290
H4C2	1.0912	H4C2	1.1014
H5C2=H6C2	1.0892	H5C1=H6C1	1.0809
O3C1C2	128.3	O3C2C1	122.8
H4C2C1	110.7	H4C2C1	117.0
H5C2C1=H6C2C1	108.4	H5C1C2	119.0
H4C2C1O3	0.0	H6C1C2	120.9
H5C2C1H4=-H6C2C1H4	121.6		
<b><math>\text{CH}_3\text{COCH}_2</math></b>			
C1C2	1.5129	C2C1O4	121.6
C1C3	1.4467	H5C2C1	109.5
O4C1	1.2291	H6C2C1=H7C2C1	110.2
H5C2	1.0869	C1C3H8	118.1
H6C2=H7C2	1.0917	H9C3H8	119.9
H8C3	1.0803	H5C2C1C3	180.0
H9C3	1.0814	H6C2C1H5=- H7C2C1H5	120.8
C2C1C3	117.9		
a) $E=-152.989163$ a.u.; b) $E=-192.240093$ a.u.			

be classified in the  $C_s$  point group. Since coupled cluster theory does not satisfy the Hellmann-Feynman theorem in the usual sense, the dipole moments were computed using MRCI/CASSCF/AVTZ. Figure 2 represents those preferred geometries.

The three radicals display internal rotation that interconvert equivalent minima separated by barriers.  $\theta_1$  and  $\theta_2$  denote the  $CH_3$  and the  $CH_2$  torsional coordinates, respectively. At the RCCSD(T) level of theory, the energy barriers were computed to be  $V_3=143.7\text{cm}^{-1}$  ( $CH_3CO$ ),  $V_2=3838.7\text{cm}^{-1}$  ( $CH_2CHO$ ), and  $V_3=161.4\text{cm}^{-1}$  and  $V_2=2727.5\text{cm}^{-1}$  ( $CH_3COCH_2$ ). The  $V_3$  barrier of  $CH_3CO$  can be compared with the experimental data of Hirota *et al.*<sup>14</sup> ( $V_3=139.958$  (18) $\text{cm}^{-1}$ ). A third coordinate,  $\alpha$  (the  $CH_2$  wagging) interacts strongly with the  $CH_2$  torsion in two of the three species. Figure 3 represents one-dimensional cuts of the ground electronic state potential energy surfaces that emphasize the torsional barriers.

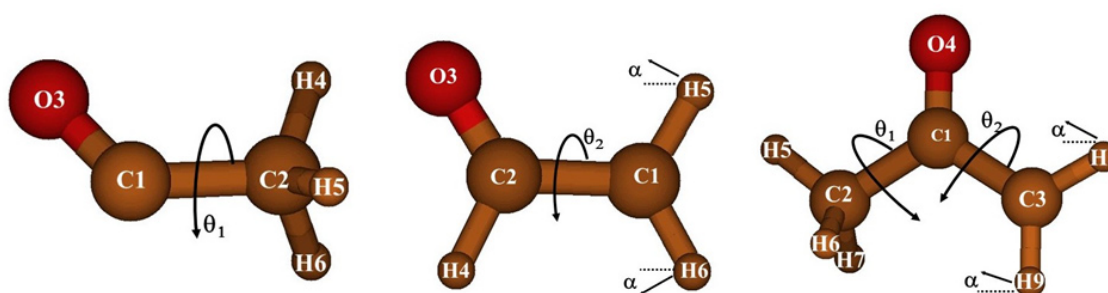


Figure 2. The preferred geometries of the  $CH_3CO$ ,  $CH_2CHO$ , and  $CH_3COCH_2$  radicals.

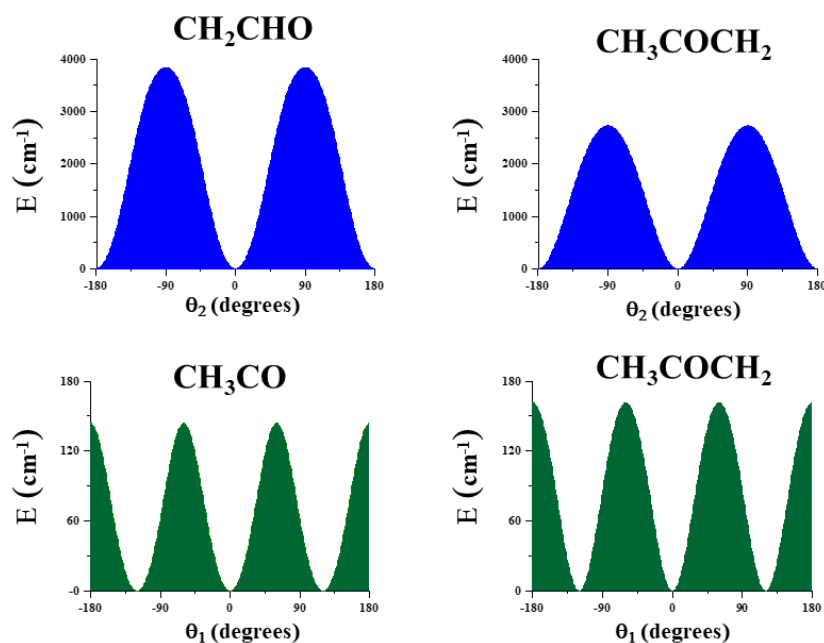


Figure 3. Internal rotation barriers.

It could be concluded that in  $\text{CH}_3\text{CO}$  and  $\text{CH}_3\text{COCH}_2$ , the methyl torsional barrier is very low ( $V_3 < 200\text{cm}^{-1}$ ). A complex distribution of the torsional energy levels can be expected. With respect to the  $\text{CH}_2$  torsion, the barrier in  $\text{CH}_3\text{COCH}_2$  is  $\sim 0.70 V_2^{\text{CH}_2\text{-CHO}}$  and of the same order of magnitude as in  $\text{CH}_3\text{OCH}_2$ <sup>43</sup>.

**Excited electronic states.** Previous theoretical and experimental works resolved doublet multiplicity character of the electronic ground states. Nevertheless, using MRCI/CASSCF/AVTZ theory, we have identified the lowest excited electronic states to assure a clean enough ground electronic state to apply the used rovibrational models. Vertical excitations are shown in Table 5 and were compared with previous experimental data<sup>22–26,29,31,33–38</sup> or data from theoretical works<sup>39,40</sup>.

The first excited electronic state of  $\text{CH}_3\text{CO}$  and  $\text{CH}_3\text{COCH}_2$  is a doublet state lying around 2 eV above the ground state. Vibronic effects are expected in the spectral region of the ground electronic state studied in this work. In the case of the  $\text{CH}_3\text{CO}$  radical, the computed value is in good agreement with experiments<sup>29</sup>. For  $\text{CH}_2\text{CHO}$ , the vertical excitation to the first excited state was computed to be 1.4 eV in agreement with the experimental value of 1.0 eV<sup>26,33,34</sup>. As a consequence, the first excited state can perturb the region of the H-stretching overtones. For the three species, the following higher excited states (doublets and quartets) lie over 4 eV.

**Ground electronic state rovibrational properties.** The vibrational energy levels have been obtained using the following formula:

$$E = \sum_i \omega_i^{\text{RCCSD}(T)\text{-F12}} \left( v_i + \frac{1}{2} \right) + \sum_{i \geq j} x_{ij}^{\text{MP2}} \left( v_i + \frac{1}{2} \right) \left( v_j + \frac{1}{2} \right) \quad (2)$$

where  $\omega_i$  represents the RCCSD(T)-F12 harmonic fundamentals and  $x_{ij}$  are the MP2 anharmonic constants. These last values were computed using VPT2 theory and harmonic force fields MP2/AVQZ (in the case of the small radicals) and MP2/AVTZ (in the case of  $\text{CH}_3\text{COCH}_2$ ).

**Table 5. Vertical excitation energies to the low-lying electronic states (in eV) computed with MRCI/CASSCF/AVTZ.**

$\text{CH}_3\text{CO}^{\text{a}}$			$\text{CH}_2\text{CHO}^{\text{b}}$			$\text{CH}_3\text{COCH}_2^{\text{c}}$		
	Calc.	Previous works		Calc.	Previous works		Calc.	
$\text{X}^2\text{A}'$	0.0	-	$\text{X}^2\text{A}''$	0.0		$\text{X}^2\text{A}''$	0.0	
$\text{A}^2\text{A}''$	2.4	2.33 <sup>29</sup> 2.6 <sup>39</sup>	$\text{A}^2\text{A}'$	1.4	1.0 <sup>26,33,34</sup>	$\text{A}^2\text{A}'$	2.2	
$\text{B}^2\text{A}'$	6.2	5.8 <sup>30</sup> (4.4-5.2) <sup>31</sup> 4.9 <sup>39</sup>	$\text{B}^2\text{A}''$	4.4	3.57 <sup>22-25,33,35,36</sup> 3.4 <sup>40</sup>	$\text{a}^4\text{A}'$	5.0	
$\text{a}^4\text{A}''$	6.3		$\text{a}^4\text{A}'$	4.9		$\text{B}^2\text{A}''$	5.7	3.4 <sup>37,38</sup> 3.5 <sup>40</sup>
$\text{b}^4\text{A}'$	6.7		$\text{C}^2\text{A}'$	5.4		$\text{b}^4\text{A}''$	6.4	
$\text{C}^2\text{A}''$	7.0	6.7 <sup>39</sup>	$\text{b}^4\text{A}''$	7.2		$\text{C}^2\text{A}'$	6.8	

a) 29 Visible Absorption Spectrum; 30 Flash photolysis and kinetic spectroscopy; 31 Ultraviolet spectrum; 39 MR(SD)CI calculations;

b) 22–25,36 Laser induced fluorescence; 26,34 Photoelectron spectroscopy; 33 Photochemical modulation spectroscopy; 35 Photodissociation spectroscopy; 40 MRCISD+Q/cc-pVDZ

c) 37,38 laser induced fluorescence; 40 MRCISD+Q/cc-pVDZ

In [Table 6](#), the computed fundamentals are compared with previous measured values in Ar<sup>16-18</sup> and p-H<sub>2</sub><sup>20</sup> matrices, and in the gas phase<sup>21-28</sup>. In addition, the intensities of the absorption transition lines from the ground state to the fundamental bands, calculated using VPT2, are also given in [Table 6](#).

The ground vibrational state rotational constants and the centrifugal distortion constants are shown in [Table 7](#). The rotational constants were computed using the RCCSD(T)-F12 equilibrium parameters of [Table 4](#) and the following equation, proposed and verified in previous studies<sup>42,65-67</sup>:

$$B_0 = B_e(\text{RCCSD(T)-F12/AVTZ}) + \Delta B_e^{\text{core}}(\text{RCCSD(T)/CVTZ}) + \Delta B_{\text{vib}}(\text{MP2/AVnZ}) \quad (3)$$

Here,  $\Delta B_e^{\text{core}}$  takes into account the core-valence-electron correlation effect on the equilibrium parameters. It can be evaluated as the difference between  $B_e(\text{CV})$  (calculated by correlating both core and valence electrons) and  $B_e(\text{V})$  (calculated by only correlating the valence electrons).  $\Delta B_{\text{vib}}$  represents the vibrational contribution to the rotational constants derived from the VPT2  $\alpha_{\text{r}}$  vibration-rotation interaction parameters.

Rotational parameters of CH<sub>3</sub>CO were compared with the experimental values of Hirota *et al.*<sup>14</sup>, whereas those of CH<sub>2</sub>CHO were compared with the data of Endo *et al.*<sup>15</sup>. The experimental work of CH<sub>3</sub>CO also details the hyperfine structure of the rotational spectrum<sup>14</sup>. For CH<sub>2</sub>CHO, the agreement between computed and measured rotational constants of B<sub>0</sub> and C<sub>0</sub> was excellent and tolerable in the case of A<sub>0</sub> (A<sub>0</sub><sup>CAL</sup>-A<sub>0</sub><sup>EXP</sup> = 95.3 MHz, B<sub>0</sub><sup>CAL</sup>-B<sub>0</sub><sup>EXP</sup> = -1.7 MHz, and C<sub>0</sub><sup>CAL</sup>-C<sub>0</sub><sup>EXP</sup> = 3.2 MHz). However, for CH<sub>3</sub>CO, the concurrence is also excellent for B<sub>0</sub> and C<sub>0</sub>, but the A<sub>0</sub> result is outside tolerance limits (A<sub>0</sub><sup>CAL</sup>-A<sub>0</sub><sup>EXP</sup> = 1147.5 MHz, B<sub>0</sub><sup>CAL</sup>-B<sub>0</sub><sup>EXP</sup> = -3.4 MHz, and C<sub>0</sub><sup>CAL</sup>-C<sub>0</sub><sup>EXP</sup> = 0.5 MHz). Generally, for many molecules, the computed B<sub>0</sub> and C<sub>0</sub> using [Equation \(3\)](#) are more accurate than A<sub>0</sub>. However, the difference expressed as A<sub>0</sub><sup>CAL</sup>-A<sub>0</sub><sup>EXP</sup> = 1147.5 MHz is too large in comparison to what was expected. Since the three rotational constants were computed simultaneously, the error could be derived from the experiments and from the effective Hamiltonian used for assignments. The authors of [Ref. 14](#) stood out that the A constant was “assumed” whereas B<sub>0</sub> and C<sub>0</sub> were fitted using the observed lines. For methyl isocyanate<sup>68</sup>, we found a similar situation, where it is proven that previous experimental works provided very contradictory A<sub>0</sub> constants.

### The far infrared region

For the three radicals, the energy levels corresponding to the large amplitude motions were computed using a variational procedure of reduced dimensionality, where the vibrational coordinates responsible for the non-rigidity were considered to be separable from the remaining vibrations. Then, an adiabatic approximation is applied on the basis of the vibrational energies. Since the method takes into consideration the minimum interconversion describing the tunneling effects in the barriers, it is more suitable for nonrigid species than VPT2, although this last theory provides a useful preliminary depiction. With VPT2, the methyl torsional fundamental of CH<sub>3</sub>CO was computed to be 82 cm<sup>-1</sup> and the fundamental frequency of the central bond torsion of CH<sub>2</sub>CHO was found at 402 cm<sup>-1</sup> (see [Table 6](#)). The CH<sub>3</sub>COCH<sub>2</sub> radical presents two interacting internal rotations which VPT2 frequencies computed to be 77 cm<sup>-1</sup> (CH<sub>3</sub> torsion) and 343 cm<sup>-1</sup> (CH<sub>2</sub> torsion). In principle, models in one-dimension (1D) or two-dimensions (2D) seems sufficient.

However, as we employed a flexible model where the remaining vibrational modes were allowed to be relaxed during the torsions, a third vibrational mode, the CH<sub>2</sub> wagging, must be considered explicitly as it is strongly coupled with the CH<sub>2</sub> torsion. Fermi interactions, predicted using VPT2, show that the separability between the CH<sub>2</sub> wagging and the CH<sub>2</sub> torsion is not suitable. Then, CH<sub>2</sub>CHO and CH<sub>3</sub>COCH<sub>2</sub> require (at least) to use 2D and a three-dimension (3D) model, respectively. For the most general case, the 3D Hamiltonian for J=0 must be defined as<sup>57-59</sup>:

$$H(\theta_1, \theta_2, \alpha) = - \sum_{i=1}^3 \sum_{j=1}^3 \left( \frac{\partial}{\partial q_i} \right) B_{q_i q_j}(\theta_1, \theta_2, \alpha) \left( \frac{\partial}{\partial q_j} \right) + V^{\text{eff}}(\theta_1, \theta_2, \alpha) \quad (4)$$

$q_i q_j = \theta_1, \theta_2, \alpha$

where  $B_{q_i q_j}(\theta_1, \theta_2, \alpha)$  are the kinetic energy parameters<sup>57-59</sup>; the effective potential is the sum of three terms:

$$V^{\text{eff}}(\theta_1, \theta_2, \alpha) = V(\theta_1, \theta_2, \alpha) + V'(\theta_1, \theta_2, \alpha) + V^{\text{ZPVE}}(\theta_1, \theta_2, \alpha) \quad (5)$$

**Table 6. Anharmonic fundamentals<sup>a,b,c</sup> (in cm<sup>-1</sup>) and intensities (I, in km/mol)<sup>d</sup>.**

CH <sub>3</sub> CO					
			Calc.	I	Obs. <sup>e</sup> [Ref]
v(a')	v <sub>1</sub>	CH <sub>3</sub> st	2988	4.80	2989.1 (19) <sup>20</sup>
	v <sub>2</sub>	CH <sub>3</sub> st	2919	3.25	2915.6(29) <sup>20</sup>
	v <sub>3</sub>	CO st	<b>1900</b>	182.79	1880.5 (100) <sup>20</sup> ; 1875 <sup>17</sup> ; 1842 <sup>18</sup>
	v <sub>4</sub>	CH <sub>3</sub> b	1427	18.41	1419.9(80) <sup>20</sup> ; 1420 <sup>17</sup>
	v <sub>5</sub>	CH <sub>3</sub> b	1331	14.82	1323.2(109) <sup>20</sup> ; 1329 <sup>17,18</sup>
	v <sub>6</sub>	HCC b	<b>1021</b>	16.21	
	v <sub>7</sub>	CC st	833	5.03	836.6(45) <sup>20</sup>
	v <sub>8</sub>	OCCb	464	5.86	468.1(28) <sup>20</sup>
v(a'')	v <sub>9</sub>	CH <sub>3</sub> st	<b>2997</b>	0.17	2990.3(42) <sup>20</sup>
	v <sub>10</sub>	CH <sub>3</sub> b	1429	7.23	1419.9(80) <sup>20</sup>
	v <sub>11</sub>	CH <sub>3</sub> b	<b>931</b>	0.03	
	v <sub>12</sub>	CH <sub>3</sub> tor	82	0.95	
CH <sub>2</sub> CHO					
v(a')	v <sub>1</sub>	CH st	3133	1.04	
	v <sub>2</sub>	CH st	3035	0.93	
	v <sub>3</sub>	CH st	<b>2813</b>	53.34	2827.91 <sup>21</sup>
	v <sub>4</sub>	CCO st	<b>1465</b>	282.82	1528 <sup>22-26</sup>
	v <sub>5</sub>	CH <sub>2</sub> b	<b>1435</b>	5.98	1486 <sup>25</sup>
	v <sub>6</sub>	OCH b	<b>1365</b>	3.76	1376 <sup>24,25</sup>
	v <sub>7</sub>	CC st	1132	56.06	1143 <sup>22,23,25-27</sup>
	v <sub>8</sub>	CC st	950	9.75	957 <sup>25</sup>
	v <sub>9</sub>	CCO b	495	15.13	500 <sup>22,23,25-27</sup>
v(a'')	v <sub>10</sub>	H <sub>4</sub> wag	954	4.57	703 <sup>25</sup>
	v <sub>11</sub>	CH <sub>2</sub> wag	729	33.77	557 <sup>25</sup>
	v <sub>12</sub>	CH <sub>2</sub> tor	402	1.05	402(4) <sup>25</sup>
CH <sub>3</sub> COCH <sub>2</sub>					
v(a')	v <sub>1</sub>	CH <sub>2</sub> st	3145	1.72	
	v <sub>2</sub>	CH <sub>3</sub> st	3074	4.61	
	v <sub>3</sub>	CH <sub>2</sub> st	3040	0.87	
	v <sub>4</sub>	CH <sub>3</sub> st	<b>2927</b>	0.34	
	v <sub>5</sub>	CO st	<b>1541</b>	472.48	1554.1 <sup>16</sup> , 1558.9 <sup>16</sup>
	v <sub>6</sub>	CH <sub>3</sub> b	<b>1449</b>	14.76	
	v <sub>7</sub>	CH <sub>2</sub> b	<b>1440</b>	17.36	1419.32 <sup>16</sup>
	v <sub>8</sub>	CH <sub>3</sub> b	1365	51.02	1377.51 <sup>16</sup>
	v <sub>9</sub>	CCH b	1243	91.05	1247 <sup>28</sup>
	v <sub>10</sub>	CCH b	1051	3.87	

CH <sub>3</sub> COCH <sub>2</sub>					
			Calc.	I	Obs. <sup>e</sup> [Ref]
	v <sub>11</sub>	CCH b	910	14.21	
	v <sub>12</sub>	CC st	813	1.67	
	v <sub>13</sub>	OCC b	521	15.98	515 <sup>28</sup>
	v <sub>14</sub>	CCCb	385	2.96	
v( a <sup>o</sup> )	v <sub>15</sub>	CH <sub>3</sub> st	2971	1.67	
	v <sub>16</sub>	CH <sub>3</sub> b	<b>1440</b>	6.25	
	v <sub>17</sub>	CH <sub>3</sub> b	1001	8.34	
	v <sub>18</sub>	CH <sub>2</sub> wag	732	28.32	
	v <sub>19</sub>	CH <sub>3</sub> b	500	1.18	
	v <sub>20</sub>	CH <sub>2</sub> tor	343	0.04	
	v <sub>21</sub>	CH <sub>3</sub> tor	77	0.18	

a st= stretching; b=bending;wag=wagging; tor=torsion.

b 16–18 Measured in Ar matrix; 20 in pH<sub>2</sub> solid; 21–28 in the gas phase.

c Emphasized in bold transitions for which important Fermi displacements are predicted.

d Intensities of the absorption transition lines from the ground state to the fundamental bands calculated using VPT<sub>2</sub>.

e Experimental uncertainties, when available, are given in parentheses in units of the last quoted digit.

**Table 7. Vibrational ground state rotational constants (in MHz) and centrifugal distortion constants corresponding to the symmetrically reduced Hamiltonian parameters (III<sup>r</sup> representation<sup>a</sup>).**

	CH <sub>3</sub> CO		CH <sub>2</sub> CHO	
	Calc.	Exp. <sup>b</sup>	Calc.	Exp. <sup>c</sup>
A <sub>0</sub>	84094.27	82946.73	66773.15	66677.85679(159)
B <sub>0</sub>	9952.09	9955.46	11445.40	11447.0460(55)
C <sub>0</sub>	9427.41	9426.95	9762.15	9758.9065(53)
Δ <sub>J</sub>	0.009448		0.009422	0.0096468(22)
Δ <sub>K</sub>	2.756343		1.312964	1.307
Δ <sub>JK</sub>	0.124574		-0.084559	-0.083045(137)
d <sub>1</sub>	-0.000948		-0.002006	0.0021215(101)
d <sub>2</sub>	0.000512		-0.000129	0.0384(26)
H <sub>J</sub>	0.000041		0.000014	
H <sub>K</sub>	0.897964		0.078700	
H <sub>JK</sub>	-0.001033		-0.000287	
H <sub>KJ</sub>	-0.630725		-0.006429	
h <sub>1</sub>	0.000004		0.000007	
h <sub>2</sub>	-0.000014		0.000001	
h <sub>3</sub>	0.000001		0.000000	

CH <sub>3</sub> COCH <sub>2</sub> (calc)				
	Calc.	Exp. <sup>b</sup>	Calc.	Exp. <sup>c</sup>
A <sub>0</sub>	10949.35		H <sub>j</sub>	0.000024
B <sub>0</sub>	9054.05		H <sub>k</sub>	-0.000014
C <sub>0</sub>	5110.78		H <sub>jk</sub>	-0.000088
Δ <sub>j</sub>	0.010134		H <sub>kj</sub>	0.000078
Δ <sub>k</sub>	0.004463		h <sub>1</sub>	0.000006
Δ <sub>jk</sub>	-0.013811		h <sub>2</sub>	0.000003
d <sub>1</sub>	-0.000763		h <sub>3</sub>	0.000002
d <sub>2</sub>	-0.000596			

a) The z-axis was selected to coincide with the x-Eckart axis in CH<sub>3</sub>CO and CH<sub>2</sub>CHO, and with the z-Eckart axis in CH<sub>3</sub>COCH<sub>2</sub>.

b) The rotational constants of Ref. 14, to be compared with our results, are given in the Principal Axes System. They were determined from the A, (B±C)/2, and D values given in the Rho-Axes System after transforming them to the Principal Axes System.

c) Ref 15.

Here,  $V(\theta_1, \theta_2, \alpha)$  represents the *ab initio* potential energy surface;  $V'(\theta_1, \theta_2, \alpha)$  is the Podolsky pseudopotential and  $V^{ZPVE}(\theta_1, \theta_2, \alpha)$  represents the zero point vibrational energy correction<sup>57-59</sup>. For the 1D and 2D model, the corresponding operators depending on  $\theta_1$  (CH<sub>3</sub>CO) or  $\theta_2$  and  $\alpha$  (CH<sub>2</sub>CHO) can be easily derived from Equation (4) removing variables. A possible analytical expression for the potential can be the product of a double Fourier series and a Taylor series:

$$V^{\text{eff}}(\theta_1, \theta_2, \alpha) = \sum \sum \sum [A_{mnl} \cos(3m\theta_1) \cos(2n\theta_2) \alpha^{2l} + A_{-mnl} \cos(3m\theta_1) \sin(2n+1)\theta_2 \alpha^{2l+1} + A_{-mnl} \sin(3m\theta_1) \sin(2n\theta_2) \alpha^{2l} + A_{-mnl} \sin(3m\theta_1) \cos(2n+1)\theta_2 \alpha^{2l+1}] \quad (6)$$

$m=0,1,2; n=0,1,2; l=0,1,2,3,4$

Similar expressions can be used for the kinetic parameters. In the most general 3D case, the Hamiltonian symmetry properties correspond to the totally symmetric representation of G<sub>12</sub><sup>69</sup>, the molecular symmetry group (MSG) of the CH<sub>3</sub>COCH<sub>2</sub> radical. Three-dimensional series corresponding to the six representations, four non degenerate A<sub>1</sub>', A<sub>1</sub>'', A<sub>2</sub>' and A<sub>2</sub>'', and two double-degenerate, E' and E'' are presented in Table 8. The MSG of the radical CH<sub>3</sub>CO is G<sub>6</sub> with three irreducible representations, and that of CH<sub>2</sub>CHO is G<sub>4</sub> with four irreducible representations A<sup>+</sup>, A<sup>-</sup>, B<sup>+</sup> and B<sup>-</sup> (based on effects of the symmetry operators (56) and E\*).

The kinetic parameters and the *ab initio* potential energy surface were determined from a grid of N selected geometries, corresponding to selected values of the independent coordinates. When 1D, 2D, or 3D models are employed, 1, 2 or 3 internal coordinates are frozen at selected values, whereas 3N<sub>a</sub>-7 (1D), 3N<sub>a</sub>-8 (2D) and 3N<sub>a</sub>-9 (3D) (N<sub>a</sub>=number of atoms) are allowed to be relaxed in all the calculated N geometries. For the CH<sub>3</sub>COCH<sub>2</sub> radical:

- a) Geometries corresponding to four values of the H5C2C1C3 dihedral angle (0°, 90°, -90° and 180°) were selected. The methyl torsional coordinate is defined as:

$$\theta_1 = (H5C2C1C3 + H6C2C1C3 + H7C2C1C3 - 360^\circ) / 3$$

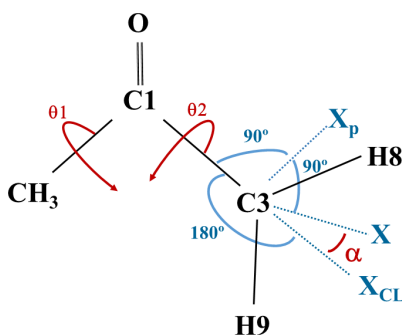
For CH<sub>3</sub>CO, the angles H<sub>x</sub>C2C1O3 (x=4,5,6) define the methyl torsional coordinate.

- b) The procedure for defining the coordinates involving the CH<sub>2</sub> group comprises 3 ghost atoms, X<sub>p</sub>, X<sub>CL</sub>, and X. X<sub>p</sub> and X defining, respectively, the torsional and wagging coordinates assuring the optimization of 3N<sub>a</sub>-8 in CH<sub>2</sub>CHO and 3N<sub>a</sub>-9 in CH<sub>3</sub>COCH<sub>2</sub> using the available GAUSSIAN<sup>47</sup> and MOLPRO software<sup>52</sup>. Figure 4 shows the distributions of real and ghost atoms in CH<sub>3</sub>COCH<sub>2</sub>.

During the geometry optimization, X<sub>p</sub> and X<sub>CL</sub> were frozen in the plane defined by the three carbon atoms; C3-X could wag outside the plane formed by C3C1C2 but remained perpendicular to C3-X<sub>p</sub>; the C3-X<sub>p</sub> and

**Table 8.** Three-dimensional wavefunctions according to MSG  $G_{12}$  ( $m, n, l=0, 1, 2, \dots$ ).

$A_1'$	$E_a'$
$\cos(3m\theta_1) \cos(2n\theta_2) \alpha^{2l}$ $\cos(3m\theta_1) \sin(2n+1)\theta_2 \alpha^{2l+1}$	$\cos(3m\pm 1)\theta_1 \cos(2n\theta_2) \alpha^{2l}$ $\cos(3m\pm 1)\theta_1 \sin(2n+1)\theta_2 \alpha^{2l+1}$
$\sin(3m\theta_1) \sin(2n\theta_2) \alpha^{2l}$ $\sin(3m\theta_1) \cos(2n+1)\theta_2 \alpha^{2l+1}$	$\cos(3m\pm 1)\theta_1 \sin(2n\theta_2) \alpha^{2l}$ $\cos(3m\pm 1)\theta_1 \cos(2n+1)\theta_2 \alpha^{2l+1}$
$A_2'$	$E_b'$
$\cos(3m\theta_1) \sin(2n\theta_2) \alpha^{2l}$ $\cos(3m\theta_1) \cos(2n+1)\theta_2 \alpha^{2l+1}$	$\sin(3m\pm 1)\theta_1 \sin(2n\theta_2) \alpha^{2l}$ $\sin(3m\pm 1)\theta_1 \cos(2n+1)\theta_2 \alpha^{2l+1}$
$\sin(3m\theta_1) \cos(2n\theta_2) \alpha^{2l}$ $\sin(3m\theta_1) \sin(2n+1)\theta_2 \alpha^{2l+1}$	$\sin(3m\pm 1)\theta_1 \cos(2n\theta_2) \alpha^{2l}$ $\sin(3m\pm 1)\theta_1 \sin(2n+1)\theta_2 \alpha^{2l+1}$
$A_1''$	$E_a''$
$\cos(3m\theta_1) \sin(2n\theta_2) \alpha^{2l+1}$ $\cos(3m\theta_1) \cos(2n+1)\theta_2 \alpha^{2l}$	$\cos(3m\pm 1)\theta_1 \sin(2n\theta_2) \alpha^{2l+1}$ $\cos(3m\pm 1)\theta_1 \cos(2n+1)\theta_2 \alpha^{2l}$
$\sin(3m\theta_1) \cos(2n\theta_2) \alpha^{2l+1}$ $\sin(3m\theta_1) \sin(2n+1)\theta_2 \alpha^{2l}$	$\cos(3m\pm 1)\theta_1 \cos(2n\theta_2) \alpha^{2l+1}$ $\cos(3m\pm 1)\theta_1 \sin(2n+1)\theta_2 \alpha^{2l}$
$A_2''$	$E_b''$
$\cos(3m\theta_1) \cos(2n\theta_2) \alpha^{2l+1}$ $\cos(3m\theta_1) \sin(2n+1)\theta_2 \alpha^{2l}$	$\sin(3m\pm 1)\theta_1 \cos(2n\theta_2) \alpha^{2l+1}$ $\sin(3m\pm 1)\theta_1 \sin(2n+1)\theta_2 \alpha^{2l}$
$\sin(3m\theta_1) \sin(2n\theta_2) \alpha^{2l+1}$ $\sin(3m\theta_1) \cos(2n+1)\theta_2 \alpha^{2l}$	$\sin(3m\pm 1)\theta_1 \sin(2n\theta_2) \alpha^{2l+1}$ $\sin(3m\pm 1)\theta_1 \cos(2n+1)\theta_2 \alpha^{2l}$

**Figure 4.** The ghost atoms defining the  $CH_2$  torsional ( $X_pC3C1C2$ ) and the wagging ( $XC3X_{CL}$ ) coordinates, in  $CH_3COCH_2$ .

$C3-X_{CL}$  “bonds” stood perpendicular and collinear to  $C3-C1$ , respectively; the real atoms H8 and H9 remained in a plane defined by the X, C3, and  $X_p$  atoms. Then, the independent  $\alpha$  and  $\theta_2$  variables and the corresponding selected values were defined as:

$$\alpha = \angle XC3X_{CL} \quad (\alpha = 0^\circ, \pm 15^\circ, \pm 30^\circ, \pm 45^\circ)$$

$$\theta_2 = X_p C3C1C2 \quad (\theta_2 = 180^\circ, 150^\circ, 120^\circ, 90^\circ)$$

A similar procedure was used for  $CH_2CHO$ .

The linear fit of the *N ab initio* energies to Equation (6) ( $R^2=0.99999$ ;  $\sigma=1.096 \text{ cm}^{-1}$  ( $CH_3COCH_2$ )) produced  $V(\theta_1, \theta_2, \alpha)$ . The kinetic parameters  $B_{\text{qij}}(\theta_1, \theta_2, \alpha)$  and the pseudopotential  $V^*(\theta_1, \theta_2, \alpha)$  were determined

using the procedure described in 57 and 58 for the N geometries and fitted to an expansion formally identical to Equation (6). To determine  $V^{ZPE}(\theta_1, \theta_2, \alpha)$ , harmonic frequencies were computed in all the N geometries. Details are shown in 56. The expansion coefficients of the effective potential are provided in Table 9. The  $A_{000}$  coefficients of the kinetic parameters are shown in Table 10. Figure 5 displays two bidimensional cuts of the 3D-effective potential of  $\text{CH}_3\text{COCH}_2$ . On the left side of the figure, the two coordinates correspond to the  $\text{CH}_3$  and  $\text{CH}_2$  torsions. On the right side, the two coordinates are those involving the  $\text{CH}_2$  group (torsion and wagging).

The energy levels were computed variationally by solving the Hamiltonian of Equation (4), using the symmetry adapted series shown in Table 8 as trial wave functions. Details concerning the classification of the levels

**Table 9. Expansion coefficients of the potential energy surfaces (in  $\text{cm}^{-1}$ )<sup>a</sup>.**

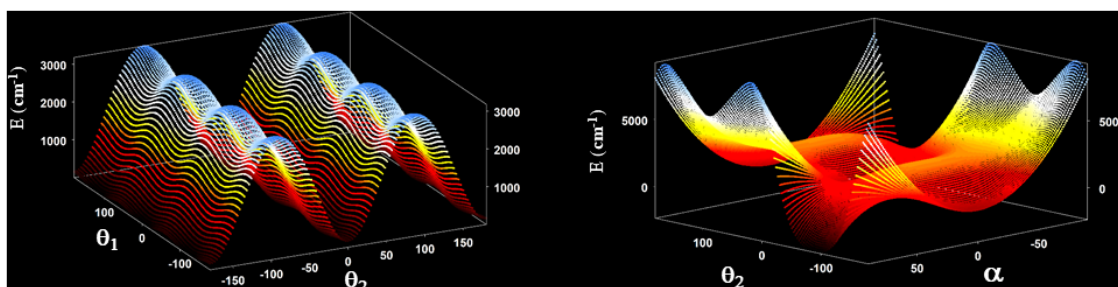
$\text{CH}_3\text{CO}$											
$A_l$	M	$A_l$	M	$A_l$	M						
66.538	0	-71.867	3	5.329	6						
$\text{CH}_2\text{COH}$											
$A_{nl}$	N	L	$A_{nl}$	N	L	$A_{nl}$	N	L			
2308.050	0	0	0.572	2	2	-4.161	-1	1			
-1958.054	2	0	$-0.6 \times 10^{-4}$	2	4	$0.7 \times 10^{-4}$	-1	3			
-55.340	4	0	-0.046	4	2	-3.838	-3	1			
38.721	6	0	$0.1 \times 10^{-4}$	4	4	$-0.11 \times 10^{-3}$	-3	3			
0.589	0	2	0.001	6	2	0.534	-5	1			
$0.10 \times 10^{-3}$	0	4	$-0.2 \times 10^{-5}$	6	4	$-0.1 \times 10^{-4}$	-5	3			
$\text{CH}_2\text{COCH}_3$											
$A_{mnl}$	N	M	L	$A_{mnl}$	N	M	L	$A_{lmn}$	N	M	L
1936.238	0	0	0	$-0.12 \times 10^{-3}$	2	0	4	$0.1 \times 10^{-5}$	4	3	4
-1432.135	2	0	0	0.069	4	0	2	0.008	-1	3	1
-61.140	4	0	0	$-0.4 \times 10^{-4}$	4	0	4	$-0.1 \times 10^{-4}$	-1	3	3
-2.543	6	0	0	0.019	6	0	2	-1.108	-3	3	1
-149.629	0	3	0	$-0.10 \times 10^{-4}$	6	0	4	$-0.5 \times 10^{-4}$	-3	3	3
-0.521	0	6	0	0.062	-1	0	1	-0.033	-5	3	1
0.379	0	0	2	0.007	-1	0	3	$0.5 \times 10^{-4}$	-5	3	3
$0.23 \times 10^{-3}$	0	0	4	2.883	-3	0	1	0.038	-2	-3	2
72.044	2	3	0	0.001	-3	0	3	$-0.1 \times 10^{-4}$	-2	-3	4
-1.843	2	6	0	-0.112	-5	0	1	-0.013	-4	-3	2
-3.507	4	3	0	$-0.5 \times 10^{-4}$	-5	0	3	$0.2 \times 10^{-5}$	-4	-3	4
-0.023	4	6	0	-0.005	0	3	2	-0.056	-6	-3	2
0.378	6	3	0	$0.1 \times 10^{-4}$	0	3	4	$0.3 \times 10^{-4}$	-6	-3	4
0.347	6	6	0	-0.001	0	6	2	0.304	1	-3	1
-73.592	-2	-3	0	-0.023	2	3	2	$0.3 \times 10^{-4}$	1	-3	3
6.280	-4	-3	0	$0.1 \times 10^{-5}$	0	6	4	-1.382	3	-3	1
0.559	2	0	2	0.003	4	3	2	$0.6 \times 10^{-3}$	3	-3	3

a)  $M=3m$ ;  $N=2n$  or  $2n+1$ ;  $L=2l$  or  $2l+1$ ;  $M \geq 0 \Rightarrow \cos 3m\theta_1$ ,  $M < 0 \Rightarrow \sin 3m\theta_1$ ;  $N \geq 0 \Rightarrow \cos N\theta_2$ ,  $N < 0 \Rightarrow \sin N\theta_2$ .

**Table 10.**  $A_{mnl}$  ( $m=0, n=0, l=0$ ) coefficients of the kinetic energy parameters (in  $\text{cm}^{-1}$ )<sup>a</sup>.

	$A_{000}(B_{aa})$	$A_{000}(B_{bb})$	$A_{000}(B_{cc})$	$A_{000}(B_{ab})$	$A_{000}(B_{ac})$	$A_{000}(B_{bc})$
$\text{CH}_3\text{CO}$	9.8515	-	-	-	-	-
$\text{CH}_2\text{CHO}$		11.9647	35.8187	-	-	0.000
$\text{CH}_3\text{COCH}_2$	5.7225	9.9603	34.3821	-0.1792	0.000	0.000

a) a= $\text{CH}_3$  torsion; b= $\text{CH}_2$  torsion; c= $\text{CH}_2$  wagging

**Figure 5.** Two dimensional cuts of the 3D potential energy surface of  $\text{CH}_3\text{COCH}_2$ .

computed in 2D and 3D can be found in 11. Table 11 collects the variational energy levels and the transitions computed using VPT2. By taking into consideration previous studies of closed-shell molecules performed with this model, we can indicate that the accuracy of the torsional fundamentals is of few wavenumber (errors  $< 5 \text{ cm}^{-1}$ ). The accuracy decreases with the energy and close to the tops of the barriers.

In  $\text{CH}_3\text{CO}$ , the A<sub>1</sub>/E splitting of the ground vibrational state was evaluated to be  $2.997 \text{ cm}^{-1}$ , as was expected given the very low torsional barrier ( $V_3=143.7 \text{ cm}^{-1}$ ) that has been computed in a very good agreement with the experimental parameter<sup>14</sup> ( $V_3=139.95 \text{ 8 (18) cm}^{-1}$ ). The methyl torsional fundamental  $\nu_{12}$  ( $1 \leftarrow 0$ ), computed to be  $82 \text{ cm}^{-1}$  with VPT2, present two components:  $104.265 \text{ cm}^{-1}$  ( $A_2 \leftarrow A_1$ ) and  $73.659 \text{ cm}^{-1}$  ( $E \leftarrow E$ ). Figure 6 can help understand the distributions of levels and subcomponents. Excitation for transitions that cannot be computed using a three-dimensional model but are expected to lie in the studied spectral region, according to the VPT2 band center positions are given in Table 11. These corresponds to the small amplitude modes  $\nu_8$  (OCC bending),  $\nu_7$  (C-C stretching), and  $\nu_{11}$  ( $\text{CH}_3$  deformation).

In  $\text{CH}_2\text{CHO}$ , the two independent fundamentals treated variationally were  $\nu_{12}$  ( $1 \text{ 0} \leftarrow 0 \text{ 0}$ ) and  $\nu_{11}$  ( $0 \text{ 1} \leftarrow 0 \text{ 0}$ ). Both were computed to be  $402 \text{ cm}^{-1}$  and  $729 \text{ cm}^{-1}$  using VPT2. The variational results were  $\nu_{12}=398.436 \text{ cm}^{-1}$  ( $A' \leftarrow A^+$ ,  $B' \leftarrow B^+$ ) and  $\nu_{11}=745.727 \text{ cm}^{-1}$  ( $A' \leftarrow A^+$ ,  $B' \leftarrow B^+$ ). The first one was in agreement with the experimental data ( $402 \pm 4 \text{ cm}^{-135}$ ) whereas large differences with the experimental work ( $557 \text{ cm}^{-135}$ ) were observed for the  $\text{CH}_2$  wagging. Both works, experimental and theoretical, need to be revisited in the future to establish the wagging mode. The separation between splitting components (in the ground and first vibrational excited states) was very small due to the height of the torsional barrier  $V_2=3838.7 \text{ cm}^{-1}$ . For  $\text{CH}_2\text{CHO}$ , the VPT2 model seems to be valid.

In  $\text{CH}_3\text{COCH}_2$ , the A/E  $\text{CH}_3$  torsional splitting of the ground vibrational state was computed to be  $0.320 \text{ cm}^{-1}$ . The two components of the three fundamentals  $\nu_{21}$  ( $1 \text{ 0 0} \leftarrow 0 \text{ 0 0}$ ),  $\nu_{20}$  ( $0 \text{ 1 0} \leftarrow 0 \text{ 0 0}$ ), and  $\nu_{18}$  ( $0 \text{ 0 1} \leftarrow 0 \text{ 0 0}$ ), were computed to be  $84.176/77.733 \text{ cm}^{-1}$ ,  $327.653/328.597 \text{ cm}^{-1}$ , and  $687.576/686.500 \text{ cm}^{-1}$ , respectively.

## Conclusions

All the possible acetone formation routes starting from 58 selected reactants were automatically generated by the programme STAR. This analysis resulted in 75 exergonic processes involving  $\text{CH}_3$ ,  $\text{CH}_3\text{CO}$  and

**Table 11. Low-lying vibrational energy levels (in  $\text{cm}^{-1}$ )<sup>a</sup> of the  $\text{CH}_3\text{CO}$ ,  $\text{CH}_2\text{CHO}$  and  $\text{CH}_3\text{COCH}_2$  radicals computed variationally or using the vibrational second order perturbation theory.** Variational energy levels are classified using the  $m$ ,  $n$  and  $l$  quanta corresponding to the  $\theta$ ,  $\theta_z$ , and  $\alpha$  coordinates according to the excitation energy. The irreducible representations are given according to the MSG  $G_6$ ,  $G_4$  and  $G_{12}$ , respectively.

$\text{CH}_3\text{CO}$ ( $G_6$ )					$\text{CH}_2\text{CHO}$ ( $G_4$ )						
$m$	Variational		VPT2		$n$	$l$	Variational		VPT2		Exp. [Ref]
0	$A_1$ $E$	0.0 2.997	ZPVE	-	0 0	$A^+$ $B^+$	0.000	ZPVE	-		
1	$A_2$ $E$	104.265 76.656	$\nu_{12}$	82	1 0	$A^-$ $B^-$	398.436	$\nu_{12}$	402	$402 \pm 4^{33}$	
2	$A_1$ $E$	132.180 185.760	$2\nu_{12}$	169				$\nu_9$	495		
3	$A_2$ $E$	379.440 272.324	$3\nu_{12}$	261	0 1	$A^-$ $B^-$	745.727	$\nu_{11}$	729	$557^{33}$	
4	$A_1$ $E$	379.849 507.146	$4\nu_{12}$	358	2 0	$A^+$ $B^+$	792.306	$2\nu_{12}$	782		
			$\nu_8$	464				$\nu_{12}\nu_9$	893		
			$\nu_{12}\nu_8$	549				$\nu_8$	950		
5	$A_2$ $E$	821.806 654.566	$5\nu_{12}$	461				$\nu_{10}$	954		
			$2\nu_{12}\nu_8$	639				$2\nu_9$	993		
			$3\nu_{12}\nu_8$	734	1 1	$A^+$ $B^+$	1123.980	$\nu_{12}\nu_{11}$	1107		
6	$A_1$ $E$	821.807 1008.819	$6\nu_{12}$	-				$\nu_7$	1132		
			$\nu_7$	833	3 0	$A^-$ $B^-$	1178.128	$3\nu_{12}$	1140		
			$\nu_{11}$	<b>931</b>				$\nu_{11}\nu_9$	1225		
			$2\nu_8$	929				$\nu_{12}\nu_8$	1348		
			$\nu_{12}\nu_7$	<b>915</b>				$\nu_{12}\nu_{10}$	1357		
			$\nu_{12}\nu_{11}$	<b>998</b>				$\nu_6$	<b>1365</b>		
								.....			
					0 2	$A^+$ $B^+$	1495.772	$2\nu_{11}$	<b>1459</b>		

a) Emphasized in bold transitions where important Fermi displacements are predicted.

$\text{CH}_3\text{COCH}_2$  radicals of which only 14 went through one or two steps and only two of them could be considered barrierless processes. The latter are the addition process  $\text{H} + \text{CH}_3\text{COCH}_2$  and  $\text{CH}_3 + \text{CH}_3\text{CO}$ . Both showed similar kinetic rates. The 75 exergonic processes are collected in Table 2. Figure 1 shows the profiles of the fourteen simplest exergonic reactions processes.

The geometrical and spectroscopic properties of some radicals involved in the processes, i.e.  $\text{CH}_3\text{CO}$ , its isomer  $\text{CH}_2\text{CHO}$ , and  $\text{CH}_3\text{COCH}_2$ , were determined by combining the two procedures and various levels of electronic structure theory. The first order properties such as geometries, equilibrium rotational constants, and harmonic fundamentals were determined using RCCSD(T). Using VPT2 and three MP2 anharmonic force

Table 11. cont.

CH <sub>3</sub> COCH <sub>2</sub> (G <sub>12</sub> )									
m n l	Variational	VPT2	m n l	Variational	VPT2				
0 0 0	A <sub>1</sub> <sup>'</sup> , A <sub>1</sub> <sup>''</sup> E <sup>'</sup> , E <sup>''</sup>	0.000 0.320	ZPVE	-	v <sub>21</sub> v <sub>19</sub>	579			
1 0 0	A <sub>1</sub> <sup>'</sup> , A <sub>1</sub> <sup>''</sup> E <sup>'</sup> , E <sup>''</sup>	84.176 78.053	v <sub>21</sub>	77	v <sub>21</sub> v <sub>13</sub>	597			
2 0 0	A <sub>1</sub> <sup>'</sup> , A <sub>1</sub> <sup>''</sup> E <sup>'</sup> , E <sup>''</sup>	126.301 147.464	2v <sub>21</sub>	146	3v <sub>21</sub> v <sub>14</sub>	622			
3 0 0	A <sub>2</sub> <sup>'</sup> , A <sub>2</sub> <sup>''</sup> A <sub>1</sub> <sup>'</sup> , A <sub>1</sub> <sup>''</sup> E <sup>'</sup> , E <sup>''</sup> E <sup>'</sup> , E <sup>''</sup>	253.926 255.131 194.827 326.007	3v <sub>21</sub>	207	2v <sub>21</sub> v <sub>19</sub>	651			
0 1 0	A <sub>2</sub> <sup>'</sup> , A <sub>2</sub> <sup>''</sup> E <sup>'</sup> , E <sup>''</sup>	327.653 328.917	v <sub>20</sub>	343	2v <sub>21</sub> v <sub>13</sub>	665			
			v <sub>14</sub>	385	0 2 0	A <sub>1</sub> <sup>'</sup> , A <sub>1</sub> <sup>''</sup> E <sup>'</sup> , E <sup>''</sup>	639.762 639.650	2v <sub>20</sub>	683
1 1 0	A <sub>1</sub> <sup>'</sup> , A <sub>1</sub> <sup>''</sup> E <sup>'</sup> , E <sup>''</sup>	414.182 407.636	v <sub>21</sub> v <sub>20</sub>	410	0 0 1	A <sub>2</sub> <sup>'</sup> , A <sub>2</sub> <sup>''</sup> E <sup>'</sup> , E <sup>''</sup>	687.576 686.820	v <sub>18</sub>	732
2 1 0	A <sub>2</sub> <sup>'</sup> , A <sub>2</sub> <sup>''</sup> E <sup>'</sup> , E <sup>''</sup>	459.559 412.652	2v <sub>21</sub> v <sub>20</sub>	468				v <sub>20</sub> v <sub>14</sub>	726
			v <sub>21</sub> v <sub>14</sub>	472				3v <sub>21</sub> v <sub>19</sub>	715
4 0 0	A <sub>1</sub> <sup>'</sup> , A <sub>1</sub> <sup>''</sup> A <sub>2</sub> <sup>'</sup> , A <sub>2</sub> <sup>''</sup> E <sup>'</sup> , E <sup>''</sup> E <sup>'</sup> , E <sup>''</sup>	507.358 507.467 479.993 527.420	4v <sub>21</sub>	260				3v <sub>21</sub> v <sub>13</sub>	725
3 1 0	A <sub>1</sub> <sup>'</sup> , A <sub>1</sub> <sup>''</sup> A <sub>2</sub> <sup>'</sup> , A <sub>2</sub> <sup>''</sup> E <sup>'</sup> , E <sup>''</sup> E <sup>'</sup> , E <sup>''</sup>	586.289 587.815 613.918 660.732	3v <sub>21</sub> v <sub>20</sub>	519				2v <sub>20</sub> v <sub>21</sub>	739
			v <sub>19</sub>	500			.....		
			2v <sub>21</sub> v <sub>14</sub>	551	0 0 2	A <sub>1</sub> <sup>'</sup> , A <sub>1</sub> <sup>''</sup>	1387.228	2v <sub>18</sub>	1459
			v <sub>13</sub>	521					

a) Emphasized in bold transitions where important Fermi displacements are predicted.

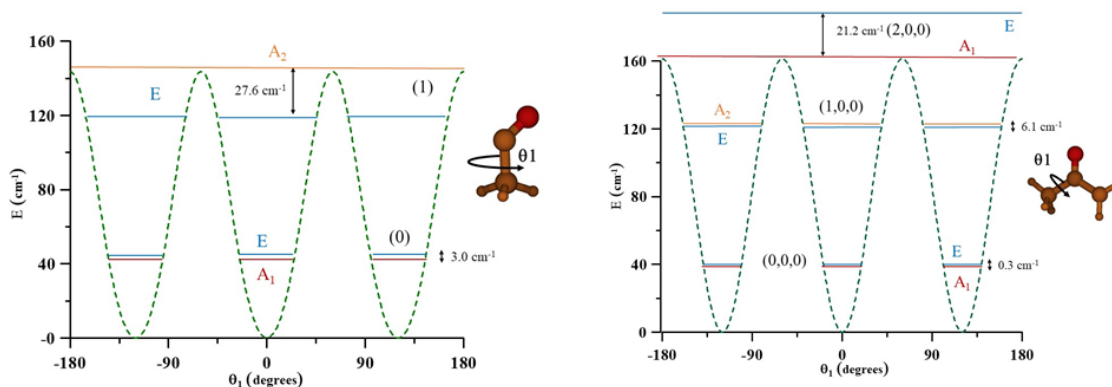


Figure 6. Methyl torsional energy levels of CH<sub>3</sub>CO and CH<sub>3</sub>COCH<sub>2</sub>.

fields, centrifugal distortion constants and anharmonic corrections for the spectroscopic parameters were computed.

As the three radicals are nonrigid species, the far infrared region was explored using a variational procedure depending on 1, 2, and 3 independent coordinates. Potential energy surfaces were computed at the RCCSD(T) levels of theory and were vibrationally corrected using MP2. This procedure takes into consideration the inter-conversion of the minima and allows to determine torsional splittings. In  $\text{CH}_3\text{CO}$ , the  $A_1/E$  splitting of the ground vibrational state, was evaluated to be  $2.997\text{ cm}^{-1}$ , as was expected given the very low torsional barrier ( $V_3=143.7\text{ cm}^{-1}$ ). The methyl torsional fundamental  $\nu_{12}$  ( $1\leftarrow 0$ ) computed to be  $82\text{ cm}^{-1}$  with VPT2, presented two components to be  $104.265\text{ cm}^{-1}$  ( $A_2\leftarrow A_1$ ) and  $73.659\text{ cm}^{-1}$  ( $E\leftarrow E$ ). In  $\text{CH}_2\text{CHO}$ , the two independent fundamentals  $\nu_{12}$  ( $1\ 0\leftarrow 0\ 0$ ) and  $\nu_{11}$  ( $0\ 1\leftarrow 0\ 0$ ) were computed to be  $\nu_{12}=398.436\text{ cm}^{-1}$  ( $A\leftarrow A^+$ ,  $B\leftarrow B^+$ ) and  $\nu_{11}=745.727\text{ cm}^{-1}$  ( $A\leftarrow A^+$ ,  $B\leftarrow B^+$ ). The separation between splitting components is very small due to the height of the torsional barrier  $V_2=3838.7\text{ cm}^{-1}$ . For  $\text{CH}_2\text{CHO}$ , the VPT2 model seems to be valid. In  $\text{CH}_3\text{COCH}_2$ , the  $A/E$   $\text{CH}_3$  torsional splitting of the ground vibrational state was computed to be  $0.320\text{ cm}^{-1}$ . The two components of the three fundamentals  $\nu_{21}$  ( $1\ 0\ 0\leftarrow 0\ 0\ 0$ ),  $\nu_{20}$  ( $0\ 1\ 0\leftarrow 0\ 0\ 0$ ), and  $\nu_{18}$  ( $0\ 0\ 1\leftarrow 0\ 0\ 0$ ), were computed to be  $84.176/77.733\text{ cm}^{-1}$ ,  $327.653/328.597\text{ cm}^{-1}$ , and  $687.576/686.500\text{ cm}^{-1}$ , respectively.

## Data availability

### Underlying data

All data underlying the results are included within the manuscript and no additional data are required.

## References

- Mellouki A, Wallington TJ, Chen J: **Atmospheric chemistry of oxygenated volatile organic compounds: impacts on air quality and climate.** *Chem Rev.* 2015; **115**(10): 3984–4014. [PubMed Abstract](#) | [Publisher Full Text](#)
- Atkinson R, Arey J: **Atmospheric degradation of volatile organic compounds.** *Chem Rev.* 2003; **103**(12): 4605–4638. [PubMed Abstract](#) | [Publisher Full Text](#)
- Singh HB, O'Hara D, Herlth D, et al.: **Acetone in the atmosphere: distribution, sources, and sinks.** *JGR Atmospheres.* 1994; **99**(D1): 1805–1819. [Publisher Full Text](#)
- Combes F, Gerin M, Wootten A, et al.: **Acetone in interstellar space.** *Astron Astrophys.* 1987; **180**: L13–L16.
- Snyder LE, Lovas FJ, Mehringer DM, et al.: **Confirmation of interstellar acetone.** *Astrophys J.* 2002; **578**(1): 245–255. [Publisher Full Text](#)
- Folkins I, Chatfield R: **Impact of acetone on ozone production and OH in the upper troposphere at high  $\text{NO}_x$ .** *JGR-Atmospheres.* 2000; **105**(D9): 11585–11599. [Publisher Full Text](#)
- Caralp F, Forst W, Hénon E, et al.: **Tunneling in the reaction of acetone with OH.** *Phys Chem Chem Phys.* 2006; **8**(9): 1072–1078. [PubMed Abstract](#) | [Publisher Full Text](#)
- Fuente A, Cernicharo J, Caselli P, et al.: **The hot core towards the intermediate-mass protostar NGC 7129 FIRS 2.** *Astron Astrophys.* 2014; **568**(A&A): A65–A94. [Publisher Full Text](#)
- Lykke JM, Coutens A, Jørgensen JK, et al.: **The ALMA-PILS survey: First detections of ethylene oxide, acetone and propanal toward the low-mass protostar IRAS 16293-2422.** *Astron Astrophys.* 2017; **597**(A&A): 53–88. [Publisher Full Text](#)
- Skouteris D, Balucani N, Ceccarelli C, et al.: **The Genealogical Tree of Ethanol: Gas-phase Formation of Glycolaldehyde, Acetic Acid, and Formic Acid.** *Astrophys J.* 2018; **854**(2): 135–144. [Publisher Full Text](#)
- Gámez V, Senent ML: **The formation of  $\text{C}_3\text{O}_3\text{H}_6$  structural isomers in the gas phase through barrierless pathways. Formation and spectroscopic characterization of methoxy acetic acid.** *Astrophys J.* 2021; **913**: 21–37. [Publisher Full Text](#)
- Senent ML, Moule DC, Smeyers YG, et al.: **A Theoretical Spectroscopic Study of the  $\tilde{A}'A_u(S_1) \leftarrow X'A_g(S_0), n \rightarrow \pi^*$  Transition in Biacetyl,  $(\text{CH}_3\text{CO})_2$ .** *J Mol Spectrosc.* 1994; **164**: 66–78. [Publisher Full Text](#)
- Senent ML, Dalbouha S: **Large amplitude motions of pyruvic acid ( $\text{CH}_3\text{-CO-COOH}$ ).** *Molecules.* MDPI, 2021; **26**(14): 4269–4282. [PubMed Abstract](#) | [Publisher Full Text](#) | [Free Full Text](#)
- Hirota E, Mizoguchi A, Ohshima Y, et al.: **Interplay of methyl-group internal rotation and fine and hyperfine interaction in a free radical: Fourier transform microwave spectroscopy of the acetyl radical.** *Mol Phys.* 2007; **105**(5–7): 455–466. [Publisher Full Text](#)
- Endo Y, Nakajima M: **Fourier-transform microwave spectroscopy of the vinoxy radical,  $\text{CH}_2\text{CHO}$ .** *J Mol Spectrosc.* 2014; **301**: 15–19. [Publisher Full Text](#)
- Hansen N, Mäder H, Temps F: **Rotational transitions of the  $\text{CH}_2\text{CHO}$  radical detected by pulsed laser photolysis-molecular beam-Fourier-transform microwave spectroscopy.** *J Mol Spectrosc.* 2001; **209**(2): 278–279. [Publisher Full Text](#)
- Jacox ME: **The reaction of F atoms with acetaldehyde and ethylene oxide. Vibrational spectra of the  $\text{CH}_3\text{CO}$  and  $\text{CH}_2\text{CHO}$  free radicals trapped in solid argon.** *J Chem Phys.* 1982; **69**(3): 407–422. [Publisher Full Text](#)
- Shirk JS, Pimentel GC: **Potential functions and the bonding in the XCO free radicals.** *J Am Chem Soc.* 1968; **90**(13): 3349–3351. [Publisher Full Text](#)
- Lin MY, Huang TP, Wu PZ, et al.: **Infrared spectra of the 1-methylvinoxide radical and anion isolated in solid argon.** *J Phys Chem A.* 2019; **123**(22): 4750–4754. [PubMed Abstract](#) | [Publisher Full Text](#)
- Das P, Lee YP: **Bimolecular reaction of  $\text{CH}_3 + \text{CO}$  in solid  $p\text{-H}_2$ : infrared absorption of acetyl radical ( $\text{CH}_3\text{CO}$ ) and  $\text{CH}_3\text{-CO}$  complex.** *J Chem Phys.* 2014; **140**(24): 244303. [PubMed Abstract](#) | [Publisher Full Text](#)
- Utkin YG, Han JX, Sun F, et al.: **High-resolution jet-cooled and room temperature infrared spectra of the  $\nu_3$  CH stretch of vinoxy radical.** *J Chem Phys.* 2003; **118**(23): 10470–10476. [Publisher Full Text](#)

22. Inoue G, Akimoto H: **Laser-induced fluorescence of the C<sub>2</sub>H<sub>3</sub>O radical.** *J Chem Phys.* 1981; **74**(1): 425–433. [Publisher Full Text](#)
23. DiMauro LF, Heaven M, Miller TA: **Laser induced fluorescence study of the B<sup>2</sup>A'' → X<sup>2</sup>A'' transition of the vinyoxy radical in a supersonic free jet expansion.** *J Chem Phys.* 1984; **81**(5): 2339–2346. [Publisher Full Text](#)
24. Wan R, Chen X, Wu F, et al.: **Observation of new vibronic transitions in the B<sup>2</sup>A''-X<sup>2</sup>A'' manifold of the CH<sub>2</sub>CHO radical.** *J Chem Phys Lett.* 1996; **260**(5–6): 539–544. [Publisher Full Text](#)
25. Brock LR, Rohlfing EA: **Spectroscopic studies of the B<sup>2</sup>A''-X<sup>2</sup>A'' system of the jet-cooled vinyoxy radical.** *J Chem Phys.* 1997; **106**(24): 10048–10065. [Publisher Full Text](#)
26. Yacovitch TI, Garand E, Neumark DM: **Slow photoelectron velocity-map imaging spectroscopy of the vinoxide anion.** *J Chem Phys.* 2009; **130**(24): 244309. [PubMed Abstract](#) | [Publisher Full Text](#)
27. Mead RD, Lykke KR, Lineberger WC: **Spectroscopy and dynamics of the dipole-bound state of acetaldehyde enolate.** *J Chem Phys.* 1984; **81**(11): 4883–4892. [Publisher Full Text](#)
28. Yacovitch TI, Garand E, Neumark DM: **Slow photoelectron velocity-map imaging of the *i*-methylvinoxide anion.** *J Phys Chem A.* 2010; **114**(42): 11091–11099. [PubMed Abstract](#) | [Publisher Full Text](#)
29. Rajakumar B, Flad JE, Gierdzak T, et al.: **Visible absorption spectrum of the CH<sub>2</sub>CO radical.** *J Phys Chem A.* 2007; **111**(37): 8950–8958. [PubMed Abstract](#) | [Publisher Full Text](#)
30. Adachi H, Basco N, James DGL: **The acetyl radical studied by flash photolysis and kinetic spectroscopy.** *J Chem Phys Lett.* 1978; **59**(3): 502–505. [Publisher Full Text](#)
31. Maricq MM, Szente JJ: **The UV spectrum of acetyl and the kinetics of the chain reaction between acetaldehyde and chlorine.** *J Chem Phys Lett.* 1996; **253**(3–4): 333–339. [Publisher Full Text](#)
32. Cameron M, Sivkumaran V, Dillon TJ, et al.: **Reaction between OH and CH<sub>2</sub>CHO.** *Phys Chem Chem Phys.* 2002; **4**(15): 3628–3638. [Publisher Full Text](#)
33. Hunziker HE, Knepe H, Wendt HR: **Photochemical modulation spectroscopy of oxygen atom reactions with olefins.** *J Photochem.* 1981; **17**(2): 377–387. [Publisher Full Text](#)
34. Alconcel LS, Deyerl HJ, Zengin V, et al.: **Structure and energetics of vinoxide and the X<sup>2</sup>(A'') and A<sup>2</sup>(A') vinyoxy radicals.** *J Phys Chem A.* 1999; **103**(46): 9190–9194. [Publisher Full Text](#)
35. Osborn DL, Choi H, Mordaunt DH, et al.: **Fast beam photodissociation spectroscopy and dynamics of the vinyoxy radical.** *J Chem Phys.* 1997; **106**(8): 3049–3066. [Publisher Full Text](#)
36. Nagai H, Carter RT, Huber JR: **Spectroscopy and dynamics of selected rotational levels in the B<sup>2</sup>A'' state of the vinyoxy radical.** *J Chem Phys Lett.* 2000; **331**(5–6): 425–432. [Publisher Full Text](#)
37. Williams S, Zingher E, Weisshaar JC: **B ← X Vibronic Spectra and B-State Fluorescence Lifetimes of Methylvinyoxy Isomers.** *J Phys Chem A.* 1998; **102**(13): 2297–2301. [Publisher Full Text](#)
38. Williams S, Harding LB, Stanton JF, et al.: **Barrier to methyl internal rotation of 1-methylvinyoxy radical in the X<sup>2</sup>(A'') and B<sup>2</sup>(A') states: experiment and theory.** *J Phys Chem.* 2000; **104**: 10131–10138.
39. Mao W, Li Q, Kong F, et al.: **Ab initio calculations of the electronic states of acetyl radical.** *J Chem Phys Lett.* 1998; **283**(1): 114–118. [Publisher Full Text](#)
40. Yamaguchi M, Inomata S, Washida N: **Multireference configuration interaction calculation of the B<sup>2</sup>A''-X<sup>2</sup>A'' transition of halogen- and methyl-substituted vinyoxy radicals.** *J Phys Chem A.* 2006; **110**(45): 12419–12426. [PubMed Abstract](#) | [Publisher Full Text](#)
41. Bennett DI, Butler LJ, Werner HJ: **Comparing electronic structure predictions for the ground state dissociation of vinyoxy radicals.** *J Chem Phys.* 2007; **127**(9): 094309. [PubMed Abstract](#) | [Publisher Full Text](#)
42. Dalbouha S, Mogren Al-Mogren M, Senent ML: **Rotational and torsional properties of various monosubstituted isotopologues of acetone (CH<sub>3</sub>-CO-CH<sub>3</sub>) from explicitly correlated ab initio methods.** *ACS Earth & Space Chem.* 2021; **5**(4): 890–899. [Publisher Full Text](#)
43. Yazidi O, Senent ML, Gámez V, et al.: **Ab initio spectroscopic characterization of the radical CH<sub>3</sub>OCH<sub>2</sub> at low temperatures.** *J Chem Phys.* 2019; **150**(19): 194102. [PubMed Abstract](#) | [Publisher Full Text](#)
44. Gámez V, Galano A, Patiño-Leyva O, et al.: **Searching tool for astrochemical reactions.** STAR v.1. [Reference Source](#)
45. Zhao Y, Schultz NE, Truhlar DG: **Design of density functionals by combining the method of constraint satisfaction with parametrization for thermochemistry, thermochemical kinetics, and noncovalent interactions.** *J Chem Theory Comput.* 2006; **2**(2): 364–82. [PubMed Abstract](#) | [Publisher Full Text](#)
46. Krishnan R, Binkley JS, Seeger R, et al.: **Self-consistent molecular orbital methods. XX. A basis set for correlated wave functions.** *J Chem Phys.* 1980; **72**(1): 650–54. [Publisher Full Text](#)
47. Frisch MJ, Trucks GW, Schlegel HB, et al.: **Gaussian 16, Revision C.01.** Gaussian, Inc., Wallingford CT, 2016.
48. Montgomery JA, Frisch MJ, Ochterski JW, et al.: **A complete basis set model chemistry. VI. Use of density functional geometries and frequencies.** *J Chem Phys.* 1999; **110**(6): 2822–2827. [Publisher Full Text](#)
49. Polyrate-version 2017-C, Zheng J, Bao JL, et al.: University of Minnesota: Minneapolis, 2017. [Reference Source](#)
50. Knizia G, Adler TB, Werner HJ: **Simplified CCSD(T)-F12 methods: theory and benchmarks.** *J Chem Phys.* 2009; **130**(5): 054104. [PubMed Abstract](#) | [Publisher Full Text](#)
51. Werner HJ, Adler TB, Manby FR: **General orbital invariant MP2-F12 theory.** *J Chem Phys.* 2007; **126**(16): 164102. [PubMed Abstract](#) | [Publisher Full Text](#)
52. Werner HJ, Knowles PJ, Manby FR, et al.: **MOLPRO.** version 2012.1, a package of ab initio programs. [Reference Source](#)
53. Kendall RA, Dunning TH, Harrison RJ: **Electron affinities of the first-row atoms revisited. Systematic basis sets and wave functions.** *J Chem Phys.* 1992; **96**(9): 6796–6806. [Publisher Full Text](#)
54. Knowles PJ, Hampel C, Werner HJ: **Coupled cluster theory for high spin, open shell reference wave functions.** *J Chem Phys.* 1993; **99**(7): 5219. [Publisher Full Text](#)
55. Woon DE, Dunning Jr TH: **Gaussian basis sets for use in correlated molecular calculations. V. Core-valence basis sets for boron through neon.** *J Chem Phys.* 1995; **103**(11): 4572–4585. [Publisher Full Text](#)
56. Barone V: **Anharmonic vibrational properties by a fully automated second-order perturbative approach.** *J Chem Phys.* 2005; **122**(1): 14108. [PubMed Abstract](#) | [Publisher Full Text](#)
57. Senent ML: **Ab initio determination of the torsional spectra of acetic acid.** *Mol Phys.* 2001; **99**(15): 1311–1321. [Publisher Full Text](#)
58. Senent ML: **Determination of the kinetic energy parameters of non-rigid molecules.** *J Chem Phys Lett.* 1998; **296**(3–4): 299–306. [Publisher Full Text](#)
59. Senent ML: **Ab initio determination of the roto-torsional energy levels of trans-1,3-butadiene.** *J Mol Spectrosc.* 1998; **191**(2): 265–275. [PubMed Abstract](#) | [Publisher Full Text](#)
60. Werner HJ, Knowles PJ: **An efficient internally contracted multiconfiguration-reference configuration interaction method.** *J Chem Phys.* 1998; **89**(9): 5803–5814. [Publisher Full Text](#)
61. Knowles PJ, Werner HJ: **An efficient method for the evaluation of coupling coefficients in configuration interaction calculations.** *Chem Phys Lett.* 1988; **145**(6): 514–522. [Publisher Full Text](#)
62. Nyden MR, Petersson GA: **Complete basis set correlation energies. I. The asymptotic convergence of pair natural orbital expansions.** *J Chem Phys.* 1981; **75**(4): 1843–1862. [Publisher Full Text](#)
63. Georgievskii Y, Klippenstein SJ: **Variable reaction coordinate transition state theory: Analytic results and application to the C<sub>2</sub>H<sub>4</sub>+H→C<sub>2</sub>H<sub>5</sub> reaction.** *J Chem Phys.* 2003; **118**(12): 5442–5455. [Publisher Full Text](#)

64. Löhle A, Kästner J: **Calculation of reaction rate constants in the canonical and microcanonical ensemble.** *J Chem Theory Comput.* 2018; **14**(11): 5489–5498.  
[PubMed Abstract](#) | [Publisher Full Text](#)
65. Georgievskii Y, Klippenstein SJ: **Long-range transition state theory.** *J Chem Phys.* 2005; **122**(19): 194103.  
[PubMed Abstract](#) | [Publisher Full Text](#)
66. Boussesi R, Senent ML, Jaidane N: **Weak intramolecular interaction effects on the torsional spectra of ethylene glycol, an astrophysical species.** *J Chem Phys.* 2016; **144**(16): 164110.  
[PubMed Abstract](#) | [Publisher Full Text](#)
67. Motiyenko RA, Margulès L, Senent ML, *et al.*: **Internal rotation of OH group in 4-hydroxy-2-butyne nitrile studied by millimeter-wave spectroscopy.** *J Phys Chem A.* 2018; **122**(12): 3163–3169.  
[PubMed Abstract](#) | [Publisher Full Text](#)
68. Dalbouha S, Senent ML, Komiha N, *et al.*: **Structural and spectroscopic characterization of Methyl Isocyanate, Methyl Cyanate, Methyl Fulminate, and Acetonitrile N-oxide using highly correlated *ab initio* methods.** *J Chem Phys.* 2016; **145**(12): 124309.  
[PubMed Abstract](#) | [Publisher Full Text](#)
69. Bunker R, Jensen P: **Molecular Symmetry and Spectroscopy.** NRC Research Press, Ottawa, 1989.  
[Reference Source](#)

# Open Peer Review

Current Peer Review Status:  

---

## Version 2

Reviewer Report 04 April 2022

<https://doi.org/10.21956/openreseurope.15691.r28871>

© 2022 Nguyen H et al. This is an open access peer review report distributed under the terms of the [Creative Commons Attribution License](#), which permits unrestricted use, distribution, and reproduction in any medium, provided the original work is properly cited.



**Ha Vinh Lam Nguyen**

CNRS, LISA, University of Paris Est Creteil, Paris, France

**Isabelle Kleiner**

CNRS, LISA, Université de Paris, Paris, France

All scientific concerns have been addressed. Some issues concerning the formatting still remain but we believe that they will be fixed once the manuscript is finalized.

**Competing Interests:** No competing interests were disclosed.

**Reviewer Expertise:** Rotational spectroscopy, microwave spectroscopy, large amplitude motions, internal rotation

**We confirm that we have read this submission and believe that we have an appropriate level of expertise to confirm that it is of an acceptable scientific standard.**

Author Response 04 Apr 2022

**Maria Luisa Senent Diez**, IEM-CSIC, Unidad Asociada GIFMAN, CSIC-UHU, Madrid, Spain

We thank the referees for the detailed work they have done and that has allowed us to significantly improve our article.

**Competing Interests:** No competing interests were disclosed.

Reviewer Report 01 April 2022

<https://doi.org/10.21956/openreseurope.15691.r28872>

© 2022 **Tasinato N.** This is an open access peer review report distributed under the terms of the [Creative Commons Attribution License](#), which permits unrestricted use, distribution, and reproduction in any medium, provided the original work is properly cited.

**Nicola Tasinato**

SMART Laboratory, Scuola Normale Superiore of Pisa, Pisa, Italy

I thank the authors for the clarifications and for the replies to my comments. The paper appears improved and hence I recommend publication in its current form.

**Competing Interests:** No competing interests were disclosed.

**Reviewer Expertise:** Experimental and theoretical spectroscopy; computational chemistry applied to structural, spectroscopic properties and chemical reactivity.

**I confirm that I have read this submission and believe that I have an appropriate level of expertise to confirm that it is of an acceptable scientific standard.**

Author Response 04 Apr 2022

**Maria Luisa Senent Diez**, IEM-CSIC, Unidad Asociada GIFMAN, CSIC-UHU, Madrid, Spain

We thank the referee for the detailed work he has done and that has allowed us to significantly improve our article.

**Competing Interests:** No competing interests were disclosed.

---

**Version 1**

Reviewer Report 20 December 2021

<https://doi.org/10.21956/openreseurope.15168.r28017>

© 2021 **Nguyen H et al.** This is an open access peer review report distributed under the terms of the [Creative Commons Attribution License](#), which permits unrestricted use, distribution, and reproduction in any medium, provided the original work is properly cited.

**Ha Vinh Lam Nguyen**

CNRS, LISA, University of Paris Est Creteil, Paris, France

**Isabelle Kleiner**

CNRS, LISA, Université de Paris, Paris, France

This manuscript presents a theoretical study of three radicals undergoing large amplitude motion(s) (LAM), either three-fold as in the acetyl radical, two-fold as in the vinoxy radical, or a

combination of both as in the 1-methylvinoxy radical with kinetic inputs to figure out reaction pathways to produce acetone from those radicals. Spectroscopic and geometrical properties such as rovibrational parameters, anharmonic vibrational transitions, and excitations to the low-lying excited states are provided to help the experimental detection of those species using rovibrational spectroscopy.

This is an excellent study of importance in the high resolution molecular spectroscopic community. Not only for quantum chemists, spectroscopic theoretical results are also of big help when trying to make preliminary assignments in the rotational and far-infrared spectra. It might also be helpful to other fields whose inputs rely on high resolution spectroscopic data, i.e. atmospheric chemistry or astrochemistry, to judge the quality and accuracy of the acquired data. The research is original, state-of-the-art, and well-performed. The manuscript is also well-written, and we have no objection to its publication, provided some revision is made, as described below. Here, we emphasize the point of view of experimentalists in the high resolution molecular spectroscopic community, using quantum chemistry results as input for spectral analysis, and of spectroscopists with expertise in modeling spectra with LAMs.

Imagining that we are aiming at studying the rotational or rovibrational spectrum of one of the three subject radicals, the first thing we will search in the paper would be the values of the rotational constants of the ground vibrational state, the geometry of the radical to have an idea about the orientation of the molecular fragment(s) undergoing the LAM, the tunneling barrier(s), and the coupling parameters between the electron spin and the rotation of the whole radical. The most important criterion for us is their accuracy, since laboratory detection of unstable species is very challenging from the experimental point of view. Purchasing the substance commercially with a reasonable purity is in no way possible, and producing it from precursors often yields a mixture of many other species which complicates very much the spectral assignment. Not taking into account the risk that the desired radical may not be produced.

Therefore, regarding the rotational constants, the method given in Eq. (3) gives quite a different quality for the *A* rotational constants of  $\text{CH}_3\text{CO}$  and  $\text{CH}_2\text{CO}$ . It was found in many benchmark calculations for small to medium-sized molecules that the *B* and *C* rotational constants are often very well-predicted when compared to the values derived experimentally (e.g. K.L.K. Lee, M. McCarthy, *J. Phys. Chem. A* **2020**, *124*, 898-910). However, since the *A* rotational constant influences very much the spectral feature which is decisive for the assignment, the prediction accuracy of this parameter is crucial. To our point of view as rotational spectroscopists, 95.3 MHz difference is rather "good" (considering the value of *A* is large) than "excellent". A difference of 1147.5 MHz is more than "outside the tolerance limits" – it is way too large to help the experimental search in such molecular systems. So the question for future high resolution spectroscopy of  $\text{CH}_3\text{COCH}_2$  is how much the theoretical prediction can be trusted. Does an additional correction necessary? The authors stated on page 9 that the discrepancy between the experimental and theoretical *A* values "could be derived from the experiments and from the effective Hamiltonian used for assignments" and gave an additional example on methyl isocyanate. This explanation is not very convincing. In the Fourier Transform microwave experiment, Hirota *et al.* only observed  $K = 0$   $\alpha$ -type transitions. It is not so much "the experiments and the effective Hamiltonian" that can explain the discrepancy, but rather the present range of *J* and *K* values available in the dataset obtained from an experiment where large radicals are hard to produce. To our knowledge, the Hirota paper is the only rotational study involving radicals with internal rotation.

Stay at this point, in Table 6, theoretical vibrational ground state rotational constants (in MHz) and centrifugal distortion constants corresponding to the symmetrically reduced Hamiltonian parameters in  $III^f$  representation are compared with experimental constants from Hirota *et al.* But it is not clear where the authors took the experimental values for those three constants from? In Table 2 of Hirota *et al.*, we found A [82756.97] and the footnote says "value in brackets are assumed", so they probably fixed the A value, not fit. Furthermore, Hirota *et al.* used the RAM method, not PAM whereas theoretical values are in PAM. Did the authors transform the RAM constants of Hirota *et al.* into PAM? For the centrifugal distortion constants, they seem to be in  $I^f$  representation in Hirota *et al.*, not in  $III^f$ . Those points should be clarified in the paper. The calculated value of  $2.997 \text{ cm}^{-1}$  (almost 90000 MHz) for the A/E splitting for  $\text{CH}_3\text{CO}$  seems very large (page 14). Can the authors compare their theoretical splitting value with the experimental splitting value observed by Hirota *et al.*?

Another point missing from the manuscript is that, as found in the paper of Hirota *et al.*, for radicals the orbital and/or spin angular momenta of the unpaired electrons are known to coupled among them and with nuclear spin angular momenta. The orbital and/or spin angular momenta interact with the overall rotational angular momentum to split the rotational spectra of these species into fine and hyperfine components. No information on the corresponding parameters is available to give a hint on the hyperfine structures appearing on the A and E states and how they affect the spectrum. If possible, such information should be added in the paper. If not, comments about the fact that this information cannot be added are necessary.

The choice of different methods to calculate the rotational constants should be clarified. The minimum energy paths are computed with DFT and 6-311+G(d,p) basis set, but it is not clear which DFT method the authors meant. The thermochemical properties are predicted with CB3-QB3, then the authors switched to M05-2X/6-311+G(d,p). The reason for choosing what to use is explained very well for the geometry optimizations and we expect the same for the calculations on energy paths and thermochemical properties.

Finally, one wonders if relative intensity calculation can be provided for fundamental or overtone vibrational modes. This information is very valuable for future experimental infrared spectroscopy.

There are some issues concerning the formatting and representation of the manuscript, which are all minor but need to be fixed:

- Page 4: "The work of Yamaguchi et al. focused on the  $\text{CH}_2\text{CHO}$ , and  $\text{CH}_3\text{COCH}_2$  radicals." One half-sentence with more details as for the previous sentence of the paragraph is needed. By the way, the comma must be deleted.
- Page 5: MP2/VQZ is given twice. What is associated with "respectively"?
- Equation 1: The letter K on the exponential term must be a small k.
- Figure 1 and 2 captions: The figure captions are very modest and need to be extended. In Figure 2 and 5, 1 and 2 after q should be subscripted. Increase the size of the letters in Figures 5 and 6 (we can barely read Figure 5 and cannot read at all Figure 6).
- The last part of Table 6 on page 12 is not correct. Calc. on the third column should be deleted and Exp. should be Calc.

- Overall, there is some formatting scheme which we would use uniquely throughout the manuscript (parameters such as rotational constants,  $s$ ,  $T$ ,  $\mu$ ,  $Q$ ,  $E$ ,  $\alpha$ ,  $\theta$ ,  $V$  and quantum numbers such as  $J$  in italic, insert a space before and after = sign, use a real minus sign and not a hyphen for minus). Table 3 caption: MHz should be MHz.
- Page 12, line -5:  $i$  and  $j$  in  $B_{ij}$  should be subscripted in relation to  $q$ .
- Table 3: H5C2--H6C2: It may be better to put H6C2 in parentheses. Similar comment for other positions.

**Is the work clearly and accurately presented and does it cite the current literature?**

Yes

**Is the study design appropriate and does the work have academic merit?**

Yes

**Are sufficient details of methods and analysis provided to allow replication by others?**

Yes

**If applicable, is the statistical analysis and its interpretation appropriate?**

Not applicable

**Are all the source data underlying the results available to ensure full reproducibility?**

No source data required

**Are the conclusions drawn adequately supported by the results?**

Yes

**Competing Interests:** No competing interests were disclosed.

**Reviewer Expertise:** Rotational spectroscopy, microwave spectroscopy, large amplitude motions, internal rotation

**We confirm that we have read this submission and believe that we have an appropriate level of expertise to confirm that it is of an acceptable scientific standard, however we have significant reservations, as outlined above.**

Author Response 10 Feb 2022

**Maria Luisa Senent Diez**, IEM-CSIC, Unidad Asociada GIFMAN, CSIC-UHU, Madrid, Spain

We thank the referee for the work he has made and the interest he has shown in the article. Their comments have allowed us to improve our article. They confirm the interest of some results. Also, we would like to emphasize that we have found very interesting the discussion about the rotational parameters. (Reviewer comments in italics)

**Comment:** Therefore, regarding the rotational constants, the method given in Eq. (3) gives quite a different quality for the A rotational constants of CH<sub>3</sub>CO and CH<sub>2</sub>CO. It was found in many benchmark calculations for small to medium-sized molecules that the B and C rotational constants are often very well-predicted when compared to the values derived experimentally (e.g. K.L.K. Lee, M. McCarthy, J. Phys. Chem. A 2020, 124, 898-910). However, since the A rotational constant influences very much the spectral feature which is decisive for the assignment, the prediction accuracy of this parameter is crucial. To our point of view as rotational spectroscopists, 95.3 MHz difference is rather “good” (considering the value of A is large) than “excellent”. A difference of 1147.5 MHz is more than “outside the tolerance limits” – it is way too large to help the experimental search in such molecular systems. So the question for future high resolution spectroscopy of CH<sub>3</sub>COCH<sub>2</sub> is how much the theoretical prediction can be trusted. Does an additional correction necessary? The authors stated on page 9 that the discrepancy between the experimental and theoretical A values “could be derived from the experiments and from the effective Hamiltonian used for assignments” and gave an additional example on methyl isocyanate. This explanation is not very convincing. In the Fourier Transform microwave experiment, Hirota *et al.* only observed K = 0 a-type transitions. It is not so much “the experiments and the effective Hamiltonian” that can explain the discrepancy, but rather the present range of J and K values available in the dataset obtained from an experiment where large radicals are hard to produce. To our knowledge, the Hirota paper is the only rotational study involving radicals with internal rotation.

**Reply:** For CH<sub>2</sub>COH, the sentence has been rewritten: “For CH<sub>2</sub>CHO, the agreement between computed and measured rotational constants of B<sub>0</sub> and C<sub>0</sub> was excellent and tolerable in the case of A<sub>0</sub> (A<sub>0</sub><sup>CAL</sup>-A<sub>0</sub><sup>EXP</sup> = 95.3 MHz, B<sub>0</sub><sup>CAL</sup>-B<sub>0</sub><sup>EXP</sup> = -1.7 MHz, and C<sub>0</sub><sup>CAL</sup>-C<sub>0</sub><sup>EXP</sup> = 3.2 MHz)” Lee and McCarthy's publication discusses stable species with an even number of electrons. These systems are easier to obtain than open shell. Our experience applying equation 3 to neutral stable molecules is that the differences between measured and calculated values are ~10 MHz (in A<sub>0</sub>) and 3-5 MHz (in B<sub>0</sub> and C<sub>0</sub>). A<sub>0</sub> usually shows a slightly lower quality. A difference of A<sub>0</sub><sup>CAL</sup>-A<sub>0</sub><sup>EXP</sup> = 95.3 MHz, B<sub>0</sub><sup>CAL</sup>-B<sub>0</sub><sup>EXP</sup> = -1.7 MHz, and C<sub>0</sub><sup>CAL</sup>-C<sub>0</sub><sup>EXP</sup> = 3.2 MHz, in a radical, as is the case of CH<sub>2</sub>CHO, can be considered a good result. However, a difference of 1147.5 MHz is not permissible. If more than one constant has a large error, it could be attributed to the chosen axis system. In this case, the rotation of the molecular frame system about an axis (i.e. changing A and B) can solve the problem. But, in our case, the CH<sub>3</sub>CO results for both C<sub>0</sub> and B<sub>0</sub> are excellent (A<sub>0</sub><sup>CAL</sup>-A<sub>0</sub><sup>EXP</sup> = 1147.5 MHz, B<sub>0</sub><sup>CAL</sup>-B<sub>0</sub><sup>EXP</sup> = -3.4 MHz, and C<sub>0</sub><sup>CAL</sup>-C<sub>0</sub><sup>EXP</sup> = 0.5 MHz). Using ab initio calculations, all three constants are obtained at once because what we are calculating are the geometries. An additional rotation about an axis can spoil one of the good constants. Then, the problem is not the selection of the axis, If only one rotational is wrong, the problem can come from two causes: one possibility is an error in the assignments. Another possibility can be that the theoretical model used for determining the Ae-A<sub>0</sub> difference neglects important contributions. Our result stands out a problem that needs a further study. In fact, one of the applications of the ab initio calculations is that can stand new undetected problems. It is not only used as a single way to determine parameters. In the paper of Hirota *et al* [14], the A constant has not been fitted. It has been “assumed”. Perhaps (we do not know), they have been used the RAM equilibrium constant Ae computed using RCCSD(T)/cc-pVTZ (this is the level employed in Ref.14). A sentence “The authors of Ref [14] stood out that the A constant was “assumed” whereas B<sub>0</sub> and C<sub>0</sub> were fitted using the observed lines” has been added to the manuscript.

**Comment:** *Stay at this point, in Table 6, theoretical vibrational ground state rotational constants (in MHz) and centrifugal distortion constants corresponding to the symmetrically reduced Hamiltonian parameters in  $III'$  representation are compared with experimental constants from Hirota et al. But it is not clear where the authors took the experimental values for those three constants from? In Table 2 of Hirota et al., we found A [82756.97] and the footnote says "value in brackets are assumed", so they probably fixed the A value, not fit. Furthermore, Hirota et al. used the RAM method, not PAM whereas theoretical values are in PAM. Did the authors transform the RAM constants of Hirota et al. into PAM? For the centrifugal distortion constants, they seem to be in  $I'$  representation in Hirota et al., not in  $III'$ . Those points should be clarified in the paper. The calculated value of  $2.997\text{ cm}^{-1}$  (almost 90000 MHz) for the A/E splitting for  $\text{CH}_3\text{CO}$  seems very large (page 14). Can the authors compare their theoretical splitting value with the experimental splitting value observed by Hirota et al.? Another point missing from the manuscript is that, as found in the paper of Hirota et al., for radicals the orbital and/or spin angular momenta of the unpaired electrons are known to couple among them and with nuclear spin angular momenta. The orbital and/or spin angular momenta interact with the overall rotational angular momentum to split the rotational spectra of these species into fine and hyperfine components. No information on the corresponding parameters is available to give a hint on the hyperfine structures appearing on the A and E states and how they affect the spectrum. If possible, such information should be added in the paper. If not, comments about the fact that this information cannot be added are necessary. The choice of different methods to calculate the rotational constants should be clarified.*

**Reply:** There is a new sentence in the section where we comment on Hirota *et al.*'s work "The experimental work of  $\text{CH}_3\text{CO}$  also details the hyperfine structure of the rotational spectrum <sup>14</sup>" With respect to the problem of the splitting, since Ref. [14] details hyperfine structure, we prefer to compare the internal rotation barrier than the splitting ( $V_3$  was computed to be  $143.7\text{ cm}^{-1}$  whereas the experimental value of Hirota et al. is  $139.958(18)\text{ cm}^{-1}$ . The energy levels computed from ab initio potential energy surfaces can have an error of  $3\text{ cm}^{-1}$ , very accurate for the ab initio calculations. A sentence "The  $V_3$  barrier of  $\text{CH}_3\text{CO}$  can be compared with the experimental data of Hirota et al [14] ( $V_3=139.958(18)\text{ cm}^{-1}$ )" has been added to the paper. The equation (3) employed for the determination of the rotational constants has been tested in many previous papers, some of them are in the list of references [Refs. 42, 67-68].  $B_e$  is computed with a very prestigious method RCCSD(T)-F12, the effect of the core electrons is added using RCCSD(T), with a core valence correlation consistent basis set, because we believe that the F12 correction is not relevant for internal shells. The less accurate part, the vibrational correction has been computed at low levels of theory to avoid a very large computational effort. Our computation of torsional levels does not consider the hyperfine structure because we do not compute the rotational structure. However, in Table 6 (now Table 7) the computed rotational parameters are given in the Principal Axes and compared to the experimental ones. The experimental rotational constants from the Rho -Axes Method have been transformed to the Principal Axes. We have eliminated the centrifugal constant of Ref.[14] shown in Table 6 (now Table 7) in the old manuscript. The comparison of the centrifugal parameters with the experimental ones is not reliable at all because only two experimental parameters were fitted as well as the A parameter was assumed. In addition, the experimental centrifugal constants are given in the A-reduced Hamiltonian and the calculated ones in the S-reduced Hamiltonian.

**Comment:** *The minimum energy paths are computed with DFT and 6-311+G(d,p) basis set, but it is not clear which DFT method the authors meant. The thermochemical properties are predicted with CB3-QB3, then the authors switched to M05-2X/6-311+G(d,p). The reason for choosing what to use is explained very well for the geometry optimizations and we expect the same for the calculations on energy paths and thermochemical properties.*

**Reply:** We use very expensive methods for spectroscopy (RCCSD(T)-F12) and modest methods for reactivity. To evaluate the procedure to obtain rotational constants is possible to use our previous papers (in the references) where we obtain an accuracy of 5 MHz (in other molecules with more standard behaviours). The equilibrium geometries (for spectroscopy) were computed using RCCSD(T)-F12/AVTZ implemented in MOLPRO. Then the equilibrium rotational constants are computed at this level of theory which is very prestigious. The correction of the core is performed at the RCCSD(T) level of theory because we believe that here the F12 correction is not relevant. The vibrational correction has been evaluated using MP2/AVTZ on the basis of the anharmonicities are less dependent on the correlation than the harmonic contributions. Whereas we tried to get very accurate spectroscopic properties, the aim of the performed description of the reactions was mainly qualitative. We agree with the referee that the kinetic parameters may be of low accuracy especially at very low temperatures. It has to be considered the number of processes studied to elucidate what are the more probable processes can be performed by comparing the different behaviours. The modest level of theory allows to distinguish between barrier and barrier-less processes. Some comments have been added to the text in the "computational methods" section.

**Comment:** *Finally, one wonders if relative intensity calculation can be provided for fundamental or overtone vibrational modes. This information is very valuable for future experimental infrared spectroscopy.*

**Reply:** Intensities have been added to Table 5 which summarizes VPT2 results. We have not determined intensities using the variational wavefunction because, as we have not experimental data, we cannot assert about the quality of the energy levels. The variational computation of intensities is very hard and we only provide intensities if we are very confident on our frequencies. If laboratories show interest in our work, and they realize that these calculations help their work, we will provide more properties. In this case, we can do intensity calculations for the bands lying in concrete in some particular spectral regions.

**Comment:** *There are some issues concerning the formatting and representation of the manuscript, which are all minor but need to be fixed: Page 4: "The work of Yamaguchi et al. focused on the CH<sub>2</sub>CHO, and CH<sub>3</sub>COCH<sub>2</sub> radicals." One half-sentence with more details as for the previous sentence of the paragraph is needed. By the way, the comma must be deleted.*

**Reply:** New sentence: "The work of Yamaguchi et al.<sup>40</sup> focused on the excited electronic states of CH<sub>2</sub>CHO and CH<sub>3</sub>COCH<sub>2</sub> radicals, was performed using multireference configuration interaction theory".

**Comment:** *Page 5: MP2/VQZ is given twice. What is associated with "respectively"? Equation 1: The letter K on the exponential term must be a small k. Figure 1 and 2 captions: The figure captions are very modest and need to be extended. In Figure 2 and 5, 1 and 2 after q should be subscripted. Increase the size of the letters in Figures 5 and 6 (we can barely read Figure 5 and cannot read at all Figure 6). The last part of Table 6 on page 12 is not correct. Calc. on the third*

*column should be deleted and Exp. should be Calc. Overall, there is some formatting scheme which we would use uniquely throughout the manuscript (parameters such as rotational constants,  $s$ ,  $T$ ,  $\mu$ ,  $Q$ ,  $E$ ,  $\alpha$ ,  $\theta$ ,  $V$  and quantum numbers such as  $J$  in italic, insert a space before and after = sign, use a real minus sign and not a hyphen for minus). Table 3 caption: MHz should be MHz. Page 12, line -5:  $i$  and  $j$  in  $B_{ij}$  should be subscripted in relation to  $q$ . Table 3:  $H5C2$ – $H6C2$ : It may be better to put  $H6C2$  in parentheses. Similar comment for other positions.*

**Reply:** Thank you very much for your help. Errors have been corrected.

**Competing Interests:** No competing interests were disclosed.

Reviewer Report 29 November 2021

<https://doi.org/10.21956/openreseurope.15168.r28019>

© 2021 Tasinato N. This is an open access peer review report distributed under the terms of the [Creative Commons Attribution License](#), which permits unrestricted use, distribution, and reproduction in any medium, provided the original work is properly cited.



### Nicola Tasinato

SMART Laboratory, Scuola Normale Superiore of Pisa, Pisa, Italy

The paper reports a theoretical study on possible formation routes of acetone under astrochemical conditions, i.e. by considering barrierless reactions. A preliminary screening has been performed and finally attention has been put on two barrierless reactions involving one elementary step. For these, rate constants have been determined using VRC-VTST.

Then, equilibrium geometries, rotational and centrifugal distortion constants have been computed for three radicals,  $\text{CH}_3\text{CO}$ ,  $\text{CH}_2\text{CO}$  and  $\text{CH}_3\text{COCH}_2$  by adopting CCSD(T)-F12 and MP2 levels of theory. For these radicals, anharmonic vibrational frequencies have been computed by using vibrational perturbation theory for the small amplitude motions (SAMs) and a variational procedure for large amplitude motions (LAMs), under the assumption that the latter ones can be decoupled from SAMs.

The methodological procedure appears adequate for the spectroscopic characterization, even though the accuracy issue is not discussed. Since computed data can be used to drive/interpret experiments, it would be interesting to point out their accuracy. Furthermore, while some wavenumbers have been experimentally measured by using different techniques (from gas-phase vibronic spectra to matrix-isolation spectroscopy), no information is available concerning infrared intensities in the gas-phase. Given the lack of experimental data, this is an important gap to fill concerning the usability of data for astrochemical detections so I am wondering why authors did not provide intensities.

Similarly, what is the estimated accuracy for the structural parameters reported in Table 3, and why dipole moment is evaluated at MRCI/CASSCF level while the remaining computations use CCSD(T) or MP2 theories? In this respect, I suggest also changing the title of Table 3 because it seems that the reported structural parameters are evaluated using MRCI/CASSCF. Please, also

write explicitly the reference wavefunction used for CCSD(T) computations of the radicals.

The methodology used for studying formation reactions can have some drawbacks that should be discussed in the text. While I do not enter on the reliability of the screening by the STAR software, I do not understand why geometries have been computed at CBS-QB3 level, that actually means B3LYP/6-31G(d) geometries, and energy profiles have been computed at M05-2X/6-311+G(d,p) level. Indeed, it has been pointed out that B3LYP geometries, especially when not augmented for dispersion interactions, cannot be reliable enough for energy evaluations, in particular for reaction complexes and transition states. In this respect, and considering the size of the investigated systems, a double-hybrid functional in conjunction with a triple-zeta basis set may appear a safer choice for reliable predictions. Furthermore, it has been demonstrated that even CBS-QB3 energies can present errors that, in turn, may cause unreliable kinetic parameters.

Concerning the computation of rotational spectroscopic parameters, what are the levels of theory used for quartic and sextic centrifugal distortions? In comparing the computed rotational constants to experimental values, it is better referring to relative errors (%) because they are probably more useful for the purpose. Indeed,  $A$  is the largest rotational constants, and hence it usually gives the largest deviations in absolute terms, but this is not necessarily true when relative errors are considered. Hence, I do not agree with the consideration that "Generally, for many molecules the computed  $B_0$  and  $C_0$  are more accurate than  $A_0$ ", and it may also be misleading for non-experts in the field. By the way, what are the tolerance limits referred to in the manuscript ("... but the  $A_0$  result is outside the tolerance limits")? Rather, I'm wondering if the cause of the deviation (about 1.4%) is related to the presence of LAMs in the  $\text{CH}_3\text{CO}$ . Indeed, LAMs can give rise to non-physical values of cubic and quartic force constants that, coupled to the fourth-order expansion of the potential energy are at the basis of the limits of VPT2 for floppy molecules. Cubic force constants are also used to evaluate the alpha-rovibrational corrections, in turn employed to obtain vibrational contributions to rotational constants. Hence, vibrational corrections can be biased by the presence of LAMs through unreliable cubic force constants. This also agrees with the fact that, the largest effects of LAMs are reported for the  $\text{CH}_3\text{CO}$  radical.

In the discussion of the variational computation of fundamental frequencies and splitting, again, what is the expected accuracy? I presume that three decimal digits represent a too optimistic accuracy so please reduce the number of significant digits accordingly (unit or one decimal at most are well suited probably) throughout all the manuscript. Furthermore, I suggest rephrasing the statement "Excitation of the low amplitude motions  $\nu_8$ ... were inserted among the  $\nu_{12}$  excitations computed variationally." (page 14). If I understood right authors are referring to combination bands (e.g.  $\nu_8 + \nu_{12}$ ) whose frequencies have been computed by mixing the variational outcome (for e.g.  $\nu_{12}$ ) with the VPT2 result (for e.g.  $\nu_8$ ). If this is the case, the  $x_{8,12}$  anharmonic constant is required for obtaining the  $\nu_8 + \nu_{12}$  frequency, but  $x_{8,12}$  may be biased as well by the presence of the  $\nu_{12}$  LAM through the cubic and quartic force constants involving this normal mode, unless the force constants involving  $\nu_{12}$  are removed. Could the authors describe in more detail the adopted procedure and, eventually, how the issue concerning anharmonic constants have been addressed? By the way, concerning this discussion, low amplitude motions should be small amplitude motions.

On inspecting Table 10, a huge difference can be observed for the variational and VPT2 frequencies of the  $4\nu_{21}$  overtone of  $\text{CH}_3\text{COCH}_2$ . This difference appears not coherent with the remaining entries of the table, so I am wondering if this is true or there is a typo in the reported

value. If real, please comment on the cause of this huge difference.

Table 11 and Figure 6 should be placed and discussed in Section "Barrierless formation processes of acetone". Furthermore, the different energy contributions to  $\Delta G$  should be detailed in Table 11 and, more importantly, activation energies should be reported. Also Figure 6 is not adequately described: some of the minimum energy paths show a very peculiar shape, in particular 3) and 8), and hence deserve to be commented.

In Table 5, several references are given for the experimental values, but it is not clear the source of some values. For example, for  $\text{CH}_2\text{CHO}$  the experimental frequency of  $\nu_4$  is reported to be  $1528\text{ cm}^{-1}$  taken from refs. 22-26, but the value reported in ref. 22 is  $1560\text{ cm}^{-1}$ . So it would be nice to have either a correspondence between the reported value and reference from which it is taken, or describe how the experimental value has been derived.

Apart from the above main points, the manuscript is in general well written although some polishing may be required, and also the text should be carefully revised to fix typos. Just to cite few of them: on page 5, VQZ (line 1) and MP2/VQZ (line 5) are reported twice; in Table 5 the experimental frequencies of  $\nu_6$  and  $\nu_9$  of  $\text{CH}_2\text{CHO}$  are missing and only references are given; Table 11: use '.' as decimal separator instead of ','.

**Is the work clearly and accurately presented and does it cite the current literature?**

Yes

**Is the study design appropriate and does the work have academic merit?**

Yes

**Are sufficient details of methods and analysis provided to allow replication by others?**

Partly

**If applicable, is the statistical analysis and its interpretation appropriate?**

Not applicable

**Are all the source data underlying the results available to ensure full reproducibility?**

Partly

**Are the conclusions drawn adequately supported by the results?**

Yes

**Competing Interests:** No competing interests were disclosed.

**Reviewer Expertise:** Experimental and theoretical spectroscopy; computational chemistry applied to structural, spectroscopic properties and chemical reactivity.

**I confirm that I have read this submission and believe that I have an appropriate level of expertise to confirm that it is of an acceptable scientific standard, however I have significant reservations, as outlined above.**

Author Response 10 Feb 2022

**Maria Luisa Senent Diez**, IEM-CSIC, Unidad Asociada GIFMAN, CSIC-UHU, Madrid, Spain

We thank the referee for the work he has made and the interest he has shown in the article. His comments have allowed us to write a new improved version of the article. They confirm the interest of some of our results. (Reviewer comments in italics)

**Comment:** *The methodological procedure appears adequate for the spectroscopic characterization, even though the accuracy issue is not discussed. Since computed data can be used to drive/interpret experiments, it would be interesting to point out their accuracy. Furthermore, while some wavenumbers have been experimentally measured by using different techniques (from gas-phase vibronic spectra to matrix-isolation spectroscopy), no information is available concerning infrared intensities in the gas-phase. Given the lack of experimental data, this is an important gap to fill concerning the usability of data for astrochemical detections so I am wondering why authors did not provide intensities.*

**Reply:** In the "computational section", some comments have been added concerning the precision of the calculations corresponding to the different sections of the paper. As the referee comments, most of the calculations are predictions. As we cannot rely on the comparison with experimental data to clarify this point, we rely on the results obtained in previous studies of molecules with more experimental data, carried out with the same methodology. Intensities have been added to Table 5 (now Table 6) which summarizes VPT2 results. We have not determined intensities using the variational wavefunction because, we have no experimental data to assess the quality of the energy levels. The variational computation of intensities is very cumbersome and we only provide intensities if we are very confident on our frequencies. If the laboratories show interest in our work, these calculations could help their work, we will provide more properties. In this case, we can calculate the intensities for the bands lying in a particular spectral region.

**Comment:** *Similarly, what is the estimated accuracy for the structural parameters reported in Table 3, and why dipole moment is evaluated at MRCI/CASSCF level while the remaining computations use CCSD(T) or MP2 theories? In this respect, I suggest also changing the title of Table 3 because it seems that the reported structural parameters are evaluated using MRCI/CASSCF. Please, also write explicitly the reference wavefunction used for CCSD(T) computations of the radicals.*

**Reply:** Our experience in the computations of the dipole moment of many molecules (particularly, when the ground state has not a singlet multiplicity character) shows that multiconfigurational methods such as MRCI produce more accurate dipole moments than monoconfigurational methods such as MP2. Nevertheless, given the lack of experimental data, there is no way for a discussion about this point although we have chosen the more prestigious procedure. Dipole moment calculations with CCSD follow more complex paths than MP2, however CCSD does not satisfy the Hellmann-Feynman theorem in the usual sense. The way is not the determination of expectation values. In addition, there is no certainty that the outcome with CCSD is better than the MRCI. For the radicals, we are using RCCSD(T) methods implemented in Molpro. As we are using default options, we have not given more explanations. The caption of Table 3 has been corrected.

**Comment:** *The methodology used for studying formation reactions can have some drawbacks*

that should be discussed in the text. While I do not enter on the reliability of the screening by the STAR software, I do not understand why geometries have been computed at CBS-QB3 level, that actually means B3LYP/6-31G(d) geometries, and energy profiles have been computed at M05-2X/6-311+G(d,p) level. Indeed, it has been pointed out that B3LYP geometries, especially when not augmented for dispersion interactions, cannot be reliable enough for energy evaluations, in particular for reaction complexes and transition states. In this respect, and considering the size of the investigated systems, a double-hybrid functional in conjunction with a triple-zeta basis set may appear a safer choice for reliable predictions. Furthermore, it has been demonstrated that even CBS-QB3 energies can present errors that, in turn, may cause unreliable kinetic parameters.

**Reply:** Whereas we tried to get very accurate spectroscopic properties, the aim of the performed description of the reactions was mainly qualitative. We agree with the referee that the kinetic parameters may be of low accuracy specially at very low temperatures. Nevertheless, we have considered a very large number of processes and we were able to elucidate the more probable reactions by comparing the thermodynamic parameters. The modest level of theory allows to distinguish between barrier and barrier-less processes. Some comments have been added to the text in the “computational methods” section.

**Comment:** Concerning the computation of rotational spectroscopic parameters, what are the levels of theory used for quartic and sextic centrifugal distortions? In comparing the computed rotational constants to experimental values, it is better referring to relative errors (%) because they are probably more useful for the purpose. Indeed, A is the largest rotational constants, and hence it usually gives the largest deviations in absolute terms, but this is not necessarily true when relative errors are considered. Hence, I do not agree with the consideration that “Generally, for many molecules the computed  $B_0$  and  $C_0$  are more accurate than  $A_0$ ”, and it may also be misleading for non-experts in the field. By the way, what are the tolerance limits referred to in the manuscript (“... but the  $A_0$  result is outside the tolerance limits”)? Rather, I’m wondering if the cause of the deviation (about 1.4%) is related to the presence of LAMs in the  $\text{CH}_3\text{CO}$ . Indeed, LAMs can give rise to non-physical values of cubic and quartic force constants that, coupled to the fourth-order expansion of the potential energy are at the basis of the limits of VPT2 for floppy molecules. Cubic force constants are also used to evaluate the alpha-rovibrational corrections, in turn employed to obtain vibrational contributions to rotational constants. Hence, vibrational corrections can be biased by the presence of LAMs through unreliable cubic force constants. This also agrees with the fact that the largest effects of LAMs are reported for the  $\text{CH}_3\text{CO}$  radical.

**Reply:** The sentence “Generally, for many molecules the computed  $B_0$  and  $C_0$  are more accurate than  $A_0$ ” refers (only) to the formulae that we employ combining RCCSD(T)-F12 equilibrium constants, with MP2/AVTZ vibrational corrections, and RCCSD(T)/CVTZ corrections of the core-electrons. Of course, this is not a general result because many authors follow other approximate procedures with other results. We have employed our method for many non-rigid molecules, and an “usual result” is that whereas disagreement with experiments are of few MHz (less than 6-7MHz) for B and C, for A, discrepancies are more relevant. We refer for some papers where we have obtained an important agreement with experiments. The formulae has been verified in many previous studies such as those described in Refs.42, 67-68. Some of these studies were achieved in collaboration with laboratories. In addition, we refer to a paper where discrepancies for the A constant are very large, but  $B_0$  and  $C_0$  where obtained with very good accuracy. In this case, the comparison was performed using experimental data from 3 different groups who provide very different experimental  $A_0$ . In particular, in the paper of Hirota *et al* [14], the A constant

has not been fitted. It has been “assumed”. Perhaps (we do not know), they have used the RAM equilibrium constant  $A_e$  computed using RCCSD(T)/cc-pVTZ (this is the level employed in Ref.14). Of course the presence of LAMs and the limit of the cubic force field computed with MP2/AVTZ introduce discrepancies. A sentence “The authors of Ref [14] have indicated that the A constant has been “assumed” whereas  $B_0$  and  $C_0$  were fitted using the observed lines” has been added to the manuscript.

**Comment:** *In the discussion of the variational computation of fundamental frequencies and splitting, again, what is the expected accuracy? I presume that three decimal digits represent a too optimistic accuracy so please reduce the number of significant digits accordingly (unit or one decimal at most are well suited probably) throughout all the manuscript. Furthermore, I suggest rephrasing the statement “Excitation of the low amplitude motions  $\nu_8$ ... were inserted among the  $\nu_{12}$  excitations computed variationally.” (page 14). If I understood right authors are referring to combination bands (e.g.  $\nu_8 + \nu_{12}$ ) whose frequencies have been computed by mixing the variational outcome (for e.g.  $\nu_{12}$ ) with the VPT2 result (for e.g.  $\nu_8$ ). If this is the case, the  $x_{8,12}$  anharmonic constant is required for obtaining the  $\nu_8 + \nu_{12}$  frequency, but  $x_{8,12}$  may be biased as well by the presence of the  $\nu_{12}$  LAM through the cubic and quartic force constants involving this normal mode, unless the force constants involving  $\nu_{12}$  are removed. Could the authors describe in more detail the adopted procedure and, eventually, how the issue concerning anharmonic constants have been addressed? By the way, concerning this discussion, low amplitude motions should be small amplitude motions.*

**Reply:** Low instead small has been corrected. A sentence has been added: “By taking into consideration previous studies of closed-shell molecules performed with this model, we can indicate that the accuracy of the torsional fundamentals is of few wavenumber (errors  $< 5 \text{ cm}^{-1}$ ). The accuracy decreases with the energy and close to the tops of the barriers. We provide 3 decimal digits because this allow distinguish the splittings. To clarify the problem, we have rewritten the cited sentence “Excitation for transitions that cannot be computed using a three-dimensional model but are expected to lie in the studied spectral region, the VPT2 band center positions are given in Table 10. These corresponds to the small amplitude modes  $\nu_8$  (OCC bending),  $\nu_7$  (C-C stretching), and  $\nu_{11}$  ( $\text{CH}_3$  deformation).

**Comment:** *On inspecting Table 10, a huge difference can be observed for the variational and VPT2 frequencies of the  $4\nu_{21}$  overtone of  $\text{CH}_3\text{COCH}_2$ . This difference appears not coherent with the remaining entries of the table, so I am wondering if this is true or there is a typo in the reported value. If real, please comment on the cause of this huge difference.*

**Reply:** It is not a typo, this is the obtained result but both theories that we are using have limitations. The  $4\nu_{21}$  was computed using the VPT2 anharmonic constants and  $\nu_{21}$  is a torsional mode. In addition, the radical has a very low barrier. Both numbers can carry out errors.

**Comment:** *Table 11 and Figure 6 should be placed and discussed in Section “Barrierless formation processes of acetone”. Furthermore, the different energy contributions to  $\Delta G$  should be detailed in Table 11 and, more importantly, activation energies should be reported. Also Figure 6 is not adequately described: some of the minimum energy paths show a very peculiar shape, in particular 3) and 8), and hence deserve to be commented.*

**Reply:** As we explain before, our aim is to identify straightforward barrier-less processes for a very large number of reactions. Table 11 lists a total of 75 processes with  $\text{DG} < 0$  of the

many that have been considered. To determine correct thermodynamic parameters for all of them or very well shaped figures is above our objectives. In addition, 73 involve several stages ( $MNES > 1$ ), which makes them very unlikely, especially at low temperatures. We do not regard the activation energies because we look for barrier-less processes. Besides, Table 11 (now Table 2) and Fig. 6 (now Fig. 1) have been included in this section. So the other tables and figures have been changed accordingly to the new enumeration.

**Comment:** *In Table 5, several references are given for the experimental values, but it is not clear the source of some values. For example, for CH<sub>2</sub>CHO the experimental frequency of  $\nu_4$  is reported to be 1528 cm<sup>-1</sup> taken from refs. 22-26, but the value reported in ref. 22 is 1560 cm<sup>-1</sup>. So it would be nice to have either a correspondence between the reported value and reference from which it is taken, or describe how the experimental value has been derived.*

**Reply:** The frequency of 1528 cm<sup>-1</sup> has been measured in the gas phase using laser induced fluorescence. We collect (if it is possible) gas phase frequencies.

**Comment:** *Apart from the above main points, the manuscript is in general well written although some polishing may be required, and also the text should be carefully revised to fix typos. Just to cite few of them: on page 5, VQZ (line 1) and MP2/VQZ (line 5) are reported twice; in Table 5 the experimental frequencies of  $\nu_6$  and  $\nu_9$  of CH<sub>2</sub>CHO are missing and only references are given; Table 11: use '.' as decimal separator instead of ','.*

**Reply:** Thank you very much for your help. Errors have been corrected.

**Comment:** *Are sufficient details of methods and analysis provided to allow replication by others?*  
Partly

**Reply:** Some explanations have been added.

**Comment:** *Are all the source data underlying the results available to ensure full reproducibility?*  
Partly

**Reply:** All the data required to assure reproducibility are available in the text with an exception that are the expansion coefficients of the torsional kinetic parameters. We provide the  $A_{000}$  coefficients which are the most significant. Remaining coefficients can alter very slightly the final frequencies.

**Competing Interests:** No competing interests were disclosed.